



HAL
open science

Study of the polymer mortar based on dredged sediments and epoxy resin: Effect of the sediments on the behavior of the polymer mortar

W. Maherzi, I. Ennahal, M. Benzerzour, Yannick Mamindy-Pajany, N.-E. Abriak

► To cite this version:

W. Maherzi, I. Ennahal, M. Benzerzour, Yannick Mamindy-Pajany, N.-E. Abriak. Study of the polymer mortar based on dredged sediments and epoxy resin: Effect of the sediments on the behavior of the polymer mortar. Powder Technology, 2020, 361, pp.968-982. 10.1016/j.powtec.2019.10.104 . hal-03225012

HAL Id: hal-03225012

<https://hal.science/hal-03225012>

Submitted on 7 Mar 2022

HAL is a multi-disciplinary open access archive for the deposit and dissemination of scientific research documents, whether they are published or not. The documents may come from teaching and research institutions in France or abroad, or from public or private research centers.

L'archive ouverte pluridisciplinaire **HAL**, est destinée au dépôt et à la diffusion de documents scientifiques de niveau recherche, publiés ou non, émanant des établissements d'enseignement et de recherche français ou étrangers, des laboratoires publics ou privés.



Distributed under a Creative Commons Attribution - NonCommercial 4.0 International License

1 **Study of the polymer mortar based on dredged sediments and epoxy resin:**
2 **Effect of the sediments on the behavior of the polymer mortar**

3
4 Walid MAHERZI, Ilyas ENNAHAL, Mahfoud BENZERZOUR, Yannick MAMINDY-PAJANY, Nor-Edine
5 ABRIAK

6 LGCgE-Laboratoire de Génie Civil et géoEnvironnement, Département Génie Civil and Environnemental, IMT
7 Lille-Douai, Univ. Lille, EA 4515, 764 BD Lahure, 59500 Douai, France

8
9 **Abstract**

10 Several studies have shown the potential of upgrading sediments in the civil engineering field. However,
11 the complexity of sediments represents a scientific challenge in terms of their management. This study
12 presents the river sediments recovery in a thermosetting matrix. The characterization results epoxy
13 mortars show the feasibility of incorporating dredged sediments up to 50% substitution rate of natural
14 sand. Moreover, according to the physic, mechanical, thermal and chemical evaluations of the
15 thermosetting matrices, it appears that the performances depend on the factors of the rate of resin and the
16 rate of sediments used. Indeed, the difference between the performances of resin mortars containing
17 sediments and mortars without sediments is reduced by a resin content equal to 18%. In comparison with
18 cementitious matrix mortars, the performances of polymeric mortars are well above. Finally, the SEM
19 observations of different formulations made it possible to explain the results observed at the macroscopic
20 scale.

21
22
23

24 **Keywords:** sediment, beneficial reuse, waste management, polymer concrete, sustainability.

25
26
27
28

30 I. Introduction

31 In France the river sediments extract represents 6 million m³ per year [1]. This accumulation gradually reduces the
32 depth of rivers and becomes a constraint for river transport. The river network of Nord-Pas-de-Calais suffers from
33 significant sedimentation, due to the low flows and slopes that characterize its hydrographic network. This
34 phenomenon is fueled by significant inputs suspended matter from urban storm water runoff, erosion of agricultural
35 soils, industrial activities and sanitation networks. Fluvial dredging sediments is mainly composed by fine particles
36 and have a specific physical and chemical characteristics compared with natural aggregates like contaminant: heavy
37 metals (Hg, As, Cr, Tl, Pb, etc.) and organic pollutant (PCB, PAH, etc.) [2,3]. These characteristics imposes a risk of
38 transfer of these to the ecosystem, the organic matter which affects the physical and mechanical properties [4] and by
39 the fact that it [5]. For this Fluvial sediments are considered as waste in accordance with national legislation.

40 A number of research studies have been carried out in order to reuse sediment as secondary raw materials, like as in
41 sub base materials for road construction [6,7,8], in cement matrices [9,10,11], in lightweight aggregates formulation
42 [12,13]. However, they have shown that the use of sediments in cementitious matrices influences the characteristics
43 of fresh concrete (rheology, setting time) [14,2,15] and hardened concrete (strength and durability) [16,17].
44 Furthermore, recently research [43] was demonstrate the feasibility of used marine and fluvial sediments to make
45 polyester matrix mortars.

46 The polymer mortar is a composite material comprises a polymeric binder and a hardener and natural mineral
47 aggregates as filler in polymeric materials, such as River Sand [28], standardized siliceous sand [33], crushed basalt
48 [34]. The polymer mortar was developed for the first time in the 50's [18], then became well known in the 70's [19].
49 Today it is shown that polymer matrix materials have the following advantages: high strength properties [22], fast
50 curing time [23], good chemical resistance [24,25] and corrosion ease of manufacture, and it has a long service life
51 and low permeability. Polymer mortars have been used in several civil engineering applications, mainly used for
52 flooring and repairing cracks in damaged concrete structures, pavements, sewage pipes, hazardous waste containers,
53 several prefabricated products such as acid tanks [20,21]. The performance of polymeric mortars depends on several
54 factors, such as resin content [26,27], the quantity and size of the aggregates [28,29], the nature and the shape of the
55 aggregates [30,69], the bonding between the particle and matrix [31]. Several studies have demonstrated the
56 feasibility of using have used waste such as recycled glass [35], foundry sand [32], fly ash [36,21,37], red mud [38],
57 waste polyethylene terephthalate (PET) [39,40], marble powder waste [41], wood flour [42] and rubber particles
58 [69]. Also, Wang et al. [69] have demonstrated that the added rubber particles can improve the mechanical
59 performance of the epoxy concrete materials, especially on compressive strength and splitting tensile strength.

60 Our research study carried out the feasibility of reusing sediments as aggregates in a thermosetting polymer matrix.
61 The mechanical strengths of a polymer mortar mainly depend on the intragranular porosity. The formulations of resin
62 mortar were optimized using the Packing Density Model. The purpose of this model is to optimize the granular
63 skeleton to reduce intragranular porosity. Once the granular skeleton was optimized, the resin was added to bind the

64 particles and at the same time to fill the residual intragranular porosity. It is noted that the epoxy resin does not
65 exhibit any significant dimensional change in hardening. Therefore, this optimization method makes it possible to
66 have a better mixture in the hardened state.

67 **II. Materials and characterization**

68 **II.1. Resin**

69 The binder used is composed by a solvent-free and transparent epoxy-based castable resin. The hardener was
70 selected with a reaction rate of between 40 minutes and 50 minutes. The epoxy resin can be mixed with different
71 fillers and will allow, according to the proportion of resin, to obtain mortars. Table 1 presents the characteristics of
72 the epoxy resin.

73 **II.2. Characterization of aggregates**

74 The sediment used in this study was provided by the waterways authority of France (Voie Navigable de France). It
75 was dredged from the Neufossé channel during the maintenance work done in 2017 (framed area in red on the Fig1).
76 The sand used is standardized sand (ISO 679 standardized sand) is natural siliceous sand, especially in the finest
77 fractions. It's clean the grains are of generally isometric and rounded shape. The sediment and sand density was
78 measured using a Micromeritics Accupycs 1330 helium pycnometer model. This test was performed in accordance
79 with standard NF EN 1097-7: (2008). The specific surface area of sediment was also measured in accordance with
80 standard NF EN ISO 18757: (2003), using a Micromeritics Autopore IV 9505 instrument. The evaluation of organic
81 matter content was carried out by the loss on ignition test according to the standard XP P94-0447: (1998) which
82 consist on the calcination at 450 ° C for 3h. The loss of mass is measured and related to the initial dry mass. The
83 methylene blue absorption test (VBS) for the evaluation of the sediment was also carried out in accordance with
84 standard NF P 94 - 068: (1998). Table 2 presents the physical characterization of the sediments. Determination of the
85 particle size is performed with an LS 13320 laser apparatus. The particle size distribution of the aggregates is shown
86 in the figure (Fig 2).

87 The mineralogical characterization of sediment and sand is carried out essentially by X-ray diffraction analysis
88 (XRD). The analysis is carried out using a device of the Siemens D5000 type and consists of a measurement of the
89 intensity and the diffraction angles pertaining to the internal atomic structuring. This is completed by an X-ray
90 fluorescence (FX) analysis to determine quantitatively the chemical elements involved. The results indicate that the
91 sediment composition consists mainly of quartz (SiO_2) with a low presence of calcite (CaCO_3). We also note the
92 presence of minor mineral phases such as albite ($\text{NaAlSi}_3\text{O}_8$), orthoclase (KAlSi_3O_8) and muscovite ($\text{KAl}_2(\text{AlSi}_3\text{O}_{10})$
93 ($\text{OHF})_2$). According to the semi-quantification carried out by X Ray diffraction, the majority clays of the sediment
94 are muscovite and illite-illite interstratified. Chlorite and kaolinite are also observed in smaller proportions. Quartz
95 and calcite are the major non-clays composing the sediment. Different families of feldspars are also present in
96 smaller quantities as well as dolomite in the form of traces. The XRD analysis highlighting the crystallized phases
97 thus proves that this sand consists exclusively of crystallized silica (Quartz) Which corresponds to the very nature of
98 the sand.

99 The results (Table 3) show that the sediment mainly contains oxygen (O), silicon (Si) and calcium (Ca). Iron (Fe)
100 and aluminum (Al) are present in significant amounts. Several elements are observed at levels close to 1%, this is the
101 case of magnesium (Mg) and potassium (K). Finally, it should be noted the presence of very low levels of sodium
102 (Na), phosphorus (P), and sulfur (S), titanium (Ti) and chlorine (Cl) in the form of traces.

103 The leaching tests were carried out in accordance with the European standard EN 12457-2: (2002). The principle of
104 the test consists in exposing the crushed material to a leachate during 24 hours, and then analyzes the obtained eluate.
105 This test was realized on the fraction of sediment with a particle size less than or equal to 4 mm and was performed
106 in triplicate. A test portion corresponding to 90 g (± 5 g) of dry mass is placed in a one-liter flask. The material of the
107 flask is chosen so as to limit as much as possible the interactions with the waste tested and as a function of the
108 substances assayed during the analysis of the eluate (in our case, it is high density polyethylene). The lixiviate used is
109 ultra-pure water. The amount of leachate to be added is determined so that the liquid / solid ratio (L / S in L / kg of
110 dry matter) is 10 ($\pm 2\%$). The flask is then shaken with a rotary shaker at 10 rpm for 24 hours (± 30 min). At the end
111 of the test, the separation of the eluate from the solid is done in 2 steps. First, the mixture is allowed to settle (for 15
112 minutes ± 5 min) and then the eluate is filtered through a 0.45 μm cellulose acetate membrane. A centrifugation step
113 can be added in case of problems. For each eluate, the pH, the conductivity and the temperature are systematically
114 measured. The results of leaching test (Table 5) show that the release in metallic trace elements is respected for all
115 the values of the inert waste thresholds. But against, the sediment is considered as non-inert and non-hazardous
116 waste, according to the decree of 12 December 2014, because the quantity of fluoride released is twice of limit value
117 of threshold. For standardized sand, the results of the batch leaching test (NF EN 12457-2) show that the
118 concentrations of metallic trace elements, anion and soluble fraction are well below the Inert material thresholds
119 (Table 4). Only barium and vanadium could be quantified and it should be noted that the released barium
120 concentration is well below the inert thresholds.

121 **II.3. Mortar manufacturing**

122 As previously indicated, the purpose of using the packing density model is to combine different granular fraction to
123 minimize the intragranular porosity in the mix [43]. This method is presented in the following.

124 ***II.3.1. Optimization of the Packing density of mixture***

125 The Packing Density Model (PDM) makes it possible to forecast the real packing density of a mixture noted ϕ
126 present with different classes from the knowledge of the energy to be used, the packing density of each component
127 and the particle size of each component. This model is based on two physical concepts:

128 The virtual packing density of the mixture Y: it is the maximum packing density that can reach a granular stack, if all
129 the grains were stored optimally. In reality, the experimental packing density is inferior to the virtual packing
130 density.

131 Clamping index (K): is a representative quantity of clamping intensity. The index is infinite so the actual mixing
132 packing density is equal to the virtual packing density.

133 Once the interactions are known, the dominant class is determined. The virtual packing density of a mixture of n
134 classes is expressed by the formula:

135
$$\gamma_i = \frac{\beta_i}{1 - \sum_{j=1}^{i-1} [1 - \beta_i + b_{ij}\beta_i(1 - 1/\beta_j)] y_j - \sum_{j=i+1}^n [1 - a_{ij}\beta_i/\beta_j] y_j}$$
 Equation 1

136 γ_i : virtual packing density when class i is dominant,

137 n : number of classes in the mixture,

138 β_i : residual packing density of class i ,

139 β_j : residual packing density of class j ,

140 y_j : volume proportion of class j in the mixture with:

141
$$y_i = \frac{V_i}{\sum_{j=1}^n V_j}$$
 Equation 2

142 a_{ij} : loosening effect exerted by a grain j in a stack of coarse grains i ,

143 b_{ij} : wall effect exerted by a large grain i in a stack of fine grains j .

144 Calculations of the packing density of the sediment are made by precisely fixing the amount of water demand in the
 145 mixtures. Measurements were made for each formulation using a Vicat device following the standard procedure
 146 specified in the standard NF EN 196-3. Depending on the water demand, the amount of added water needs to allow a
 147 needle penetration depth of 6 mm. This amount of water allows a state of normal consistency of the dough, which
 148 corresponds to the maximum filling density of the material. The relationship between the maximum packing density
 149 and the water demand of a material is given by [44]

150
$$C = \frac{1000}{1000 + M_v \frac{M_e}{M_p}}$$
 Equation 3

151 Where M_v is the density of the powder (kg/m^3), and M_e and M_p are the masses of water and powder respectively
 152 (kg).

153 Furthermore, understanding the behaviour of a mixture requires the knowledge of its packing density. Indeed, there
 154 is a direct relationship between packing density and porosity. The latter significantly affects the mechanical
 155 properties, durability, and water absorption. The relationship between the maximum packing density and the porosity
 156 of a material is given by:

157
$$n = 1 - C$$
 Equation 4

158 Where n is the porosity and C is the packing density of the mix.

159
 160 Measurement of the packing density of sand is made with the shaking table, the test consists of placing a sample of
 161 sand in a mould under the constraint of a piston, and to apply to all the mechanical shake causing rearrangement of
 162 the grains, and thus compaction of the sample, the measurement is then that of the apparent density of the sample,
 163 which makes it possible to calculate the packing density. The packing density is calculated according to the
 164 following formula [45]

165
$$C = \rho_a / \rho_{rd}$$
 Equation 5

166 With

167 ρ_{rd} (g/cm^3) = real density in the sense of the standard NF EN 1097-6

168 ρ_a (g/cm^3) = Apparent density of the material.

169

170 Fig 3 shows the variation of the packing density of the mixtures as a function of the percentage of the sediment. It is
171 found that the optimal packing density is 0.7885 which correspond of percentage of 20% of the sediment and 80% of
172 the sand. From this curve (Fig. 3) two mixtures were selected for the rest of the study. The first one constitutes 30%
173 sediment and 70% sand, and has a packing density of 0.7805, which is very close to the max value. It was noted
174 PMxSed30. the second one constitutes 50% sand and 50% sediment, and has a packing density of 0.7443. it was
175 noted PMxSed50. For both mixtures the amount of the binder is varied between 12% and 25%. It is found that for the
176 mixture of PMxSed30 the porosity is 21.95% and for the mixture PMxSed50 is 25.57%. Table 5 shows PMxSed30
177 and PMxSed50 formulations tested. The constituents are stored according to the manufacturer's instructions or the
178 rules of art. the sand was dried at 105 ° C for 24 hours and the sediment at 60 °C for more than 72 hours to reduce
179 the moisture content. After drying the sediment, it was necessary to crush it and sift it in 2 mm sieve. The resin was
180 stored in a temperature-controlled room. The base product was mixed with the hardener in a first bucket for 3
181 minutes until a uniform mixture was obtained. In a second bucket, the charges based on sand and sediment were
182 mixed. The binder was inverted into a second container and knead again for 6 minutes. Than the mineral charges
183 were added to the binder in 2 parts. Finally, the molds are filled in two layers, and each layer is compacted using the
184 impact table (60 shots). The polymer concrete samples were demolded after 24 h and cured in air at 25 ° C and 48%
185 RH.

186 **II.4. Experimental tests**

187 ***II.4.1. The apparent density***

188 It is defined as the density of one cubic meter of the material comprising the voids of the particles as well as those
189 between particles. The apparent density of a granular material depends on its degree of compaction. It is expressed
190 by the following relation $\rho = M_s/V_t$ where V_t is the total volume and M_s its dry mass.

191 ***II.4.2. Mechanical tests***

192 To evaluate the strength of the polymer mortar, unconfined compression (UCS) and three-point bending tests were
193 performed on 40 x 40 x 160 mm samples, according to the requirements of standard NF EN 196-1. Polymer mortar
194 were conserved at a temperature of 20°C± 2 °C and relative humidity maintained at 50% at least. The compression
195 tests were carried out with a load increase of 2400 N/s ± 200 N/s. The three-point bending tests were performed with
196 a speed loading of 50 N/s ± 10 N /s. Otherwise the dynamic modulus of elasticity has also been measured by Grindo-
197 sonic frequency analyzer on 40 x 40 x 160 mm specimens.

198 ***II.4.3. Porosity***

199 Porosity by mercury intrusion was measured using mercury porosimetry. This technique provides rapid access to
200 pore distribution with good accuracy in the range of 3 nm to 360 µm and the mercury pressure range is 30000 psi
201 (206 MPa).

202 ***II.5.4. The absorption of water***

203 The absorption of water is followed over time by simple gravimetric measurement. The formula for calculating the
204 mass gain is:

$$205 \quad \text{gain mass (\%)} = \frac{M(t) - M(0)}{M(0)} * 100$$

206 Where M(t) is the mass of the MBR after immersion for a time "t" and M (0) the initial mass of the specimen in the
207 dry state.

208 ***II.5.5. Linear thermal expansion***

209 The experimental tests were carried out in accordance with standard NF EN ISO 10545-8 on three test pieces of each
210 formulation. The samples were dried at a constant temperature (110 ± 5 ° C) to constant mass and then introduced
211 into a desiccator to cool to room temperature.

212 ***II.5.6. The thermal shock resistance test***

213 Was carried out on three samples (80 mm x 40 mm x 40 mm) of each formulation. The specimen subjected to 10
214 cycles during which the temperature varies between 15 ° C and 145 ° C. according to EN ISO 10545-9. The visible
215 defects on the specimens were identified by examining them with the naked eye.

216 ***II.5.7. The chemical resistance***

217 Test was carried out in accordance with EN 10545-13. The following solutions were used:

- 218 • 3% hydrochloric acid solution (volumetric percentage).
- 219 • 18% hydrochloric acid solution (volumetric percentage).
- 220 • Potassium hydroxide (KOH) solution, 30 g / l.
- 221 • Potassium hydroxide (KOH) solution, 100 g / l.

222 The test specimens were immersed in the citric acid solution and kept in the laboratory for 24 hours according to the
223 standard. For the hydrochloric acid and potassium hydroxide resistance test, the specimens were immersed for 96
224 hours.

225 **III. Results and discussion**

226 ***III.1. The apparent density***

227 The figure (4 a) shows the evolution of Polymer mortars PMx density for the curing time of 7, 14 and 28 days. We
228 note that the density was range between 1689.23 kg / m³ and 1891.12 kg / m³. The increase in the density observed
229 during the curing time for the polymer mortar (PMx) can be attributed to the increase of the crosslinking density of
230 the epoxy polymer binder, which already related in a previous study on the micro epoxy concrete polymer [46]. At
231 28 days of curing, it is noted that the density of the polymer mortar increased by 1.28% for the mass fraction of the

232 binder range from 12% to 14% and then decreases by 2.38%, 3.68%, 1.01%, 2.33% and 0.63% respectively when the
233 mass fraction of the binder increases between 14% and 25%. There is an optimum of resin quantity (14%) which
234 makes it possible to have a maximum density of PMx mortars. This can be explained by the fact of increasing the
235 mass fraction of the resin (density equal to 1100 kg/m³) implies a decrease in the granular mass fraction (density
236 equal to 2600 kg/m³), causing a decrease in the density of the mixture. The graph (4-b) and (4-c) shows the evolution
237 of polymer mortars density PMxSed30 and PMxSed50 for 7 days, 14 days, and 28 days. At 28 days curing time, the
238 density of all mixtures incorporating sediment was range between 1500 kg/m³ and 2000 kg/m³. It is noted that the
239 density decreases in day 14 except for the PM16Sed30 and PM20Sed30 formulations. It is noted that the density
240 decreases in day 14 except for the PM16Sed30 and PM20Sed30 formulations. Unlike polymer mortars without
241 sediments (PMx), the density increases with the increase in the mass rate of sediments. It is observed that the density
242 for the formulations PM12Sed50 and PM14Sed50 is decreased to 1.45% and 3.57%, for PMxSed50 for x equal 18
243 and 25 increased by 1.87% and 1.63% respectively. It is observed that the density of the polymer mortar
244 (PMxSed50) at 28 days bound to the mass fraction of the binder. Figure 5 shows the density of polymer mortars at
245 28 days. We note that the density of the PMx polymer mortar for the mass fraction is 12, 14 and 16 % are higher than
246 that of the polymer mortar PMxSed30 and PMxSed50. The mass fractions of the binder equals 18% and it is
247 observed that the density of the PMx polymer mortar is low compared to PMxSed30. It is observed that the density is
248 related to the amount of binder and sediment. From the 16% of the mass fraction of the binder, the density of the
249 polymer mortar PMx decreases, unlike the polymer mortars based on the sediment. For comparative purposes,
250 several study [33,39,41,47], where they optimized the polymer mortar or concrete, showed that the incorporation of
251 fillers (marble powder, cork granules, sand) increased the density of polymer concrete until some mass fractions of
252 the binder which causes a drop in the latter.

253 *III.2. Compressive test*

254 Figure (Fig 6-a) shows the evolution of the compressive strength of the PMx formulation for 7 days, 14 days and 28
255 days. All the test results were calculated by the average of three measurements for each type of samples. It's notes
256 that the compressive strength increases for all mass fractions of resin as a function of time. It is observed that
257 between 7 days and 28 days will not have much difference in compressive strength. Several studies [48,49,50] shown
258 that the compressive strength of the polymer concrete becomes almost constant and that it reaches three-thirds of its
259 maximum compressive strength in the first days of curing. It is observed that compressive strength increases when
260 the content of the binder increases between 12 and 18 %. Hereafter 18% of binder content the compressive strength
261 decreases gradually. This can be explained by fact that appearance of saturated zone with epoxy binder, which
262 decreases intragranular interaction and deteriorate consequently the mechanical properties of the mortar PMx. The
263 Fig 6-b shows the evolution of the compressive strength of the PMxSed30 formulation for different percentages of
264 mass fraction for 7 days, 14 days and 28 days. It is noted that compressive strength increases over time for all
265 PMxSed30 formulations except for the PM18Sed30 formulation. It notes that the compressive strength of the
266 polymer mortar PMxSed30 increases as the amount of resin content increases. It is observed that the compressive
267 strength is almost stable for 28 days. Note that the compressive strength between the mortar PM16Sed30 and

268 PM18Sed30 increases by 118%. This can be mainly due to the reduction of the internal porosity of the polymer
269 mortars. In fact, it is noted that the porosity decreases from 15% to about 5% between the mortars PM16Sed30 and
270 PM18SED30, respectively. Fig. 7 shows the compressive strength of the mortars PMx, PMxSed30 and PMxSed50 in
271 28 days, we take note that:

- 272 • The compression strength of masse fractions equal to 12; 14; 16; 18; 20 and 25 of the PMxSed30
273 formulation is small compared to the mortar PMx of the same mass fraction with a percentage difference of
274 74.59%, 75.89%, 67.11%, 33.86%, 20.14% and 3.32%, respectively.
- 275 • The compression strength of masse fractions equal to 12, 14, 16, 18, 20 and 25 of the PMxSed50
276 formulation is small compared to the mortar PMx of the same mass fraction with a percentage difference of
277 89.9%, 92.2%, 84.65%, 74.53%, 42.51% and 11.51%, respectively.
- 278 • The compression strength of masse fractions equal to 12; 14; 16; 18; 20 and 25 of the PMxSed50
279 formulation is lower compared to the mortar PMxSed30 of the same mass fraction with a percentage
280 difference of 52.03%, 67.68%, 53.33%, 61.49%, 28.02% and 8.47%, respectively.

281 These differences can be expressed by several factors by the lack of the amount of binder required to coat the
282 aggregates and fill the voids between the aggregates. The increase in the binder content allows a better coating of the
283 aggregates and leads to completely filling the gaps between the aggregates. Several previous study [51,36,52,53]
284 confirm these observations. indeed, it is observed that the compressive strength decreases when the amount of the
285 sediment increases, and the amount of fines affects the mechanical properties from the amount added to the matrix.
286 Another explanation for this decrease can be due to a high capacity to absorb water. In fact, during the mixing with
287 the resin, sediments absorbed a certain quantity of the resin. Several studies have shown the influence of
288 granulometry on the properties of the polymer mortar also as reported in the literature [54]. The granular mixture in
289 the mortar affects the compressive strength. The granular mixture must be mixed in a manner and a minimum void
290 content and maximum bulk density [55]. The smaller particles have a larger area. Therefore, the specific area of the
291 sediment is larger compared to the sand implies a higher dosage of resin. in the literature [56,57,58] has shown the
292 effect of the specific surface area on the amount of resin and on the compressive strength. This difference in
293 compressive strength between mortars can be explained by the difference in the type of aggregates. Indeed, Fu et al.
294 [53] has shown that the type of aggregates affect compressive strength. The bond between the charge and the matrix
295 and the amount of charges in the matrix are two important factors that also affect the mechanical properties [53]. For
296 well-matrix-bound fillers, the stress applied to the mortar can be efficiently transferred to the particles from to the
297 matrix.

298 ***III.3. Flexural strength***

299 The figure (8-a, b and c) shows the flexural strength of the mortar PMx, PMxSed30 and PMxSed50 formulation of
300 different resin mass fractions for 7 days, 14 days and 28 days. For the PMx formulations, it is observed that the
301 resistance increases with time for all the mass fractions. It should be noted that flexural strength increases with the
302 increasing resin content. By 25% of the mass fraction of the resin, the flexural strength decreased slightly. The

303 flexural strength of the PMx mortar increased by 54.11% as the mass fraction of the binder increased from 12% to
304 14%. From the mass fraction, 14% the flexural strength between 20.59 MPa and 25.89 MPa. At 28 days, the flexural
305 strength of 4.8 MPa to 7.96 MPa was observed for the PM12Sed30, PM14Sed30 and PM16Sed30 mortars. For
306 mortars PM18Sed30 and PM20Sed30, the flexural strength is between 16.89 MPa and 18.03 MPa. For mortar
307 PM25Sed30 is 26.03 MPa. Otherwise, at 28 days, the flexural strength of PM12Sed50, PM14Sed50, PM16Sed50,
308 PM18Sed50, PM20Sed50 and PM25Sed50 equals 1.71 MPa, 4.65 MPa, 4.93 MPa, 8.91 MPa, 11.94 MPa and 20.05
309 MPa respectively. It is observed that for all formulations (PMx, PMxSed30 and PMxSed50) the flexural strength is
310 related to the resin content. Figure 9 shows the flexural strength of the formulations: PMx; PMxSed30 and
311 PMxSed50 in twenty-eight days. it is found that the flexural strength of PMx is greater than that of PMxSed30 and
312 PMxSed50 formulations for a mass fraction equal to: 12; 14; 16; 18 and 20%.

313 It follows from the foregoing it is noted that:

- 314 • The flexural strength of mass fraction equal to 12; 14; 16; 18; 20 and 25% of the PMxSed30 formulations
315 decreased by 64.07; 67.45; 66.12; 28.97 and 30.35% compared to the PMx formulation respectively.
- 316 • The flexural strength of mass fraction equal to 12; 14; 16; 18; 20 and 25% of the PMxSed50 formulation
317 decreased by 87.20; 76.05; 62.53; 28.97, 53.88 and 20.75% compared to the PMx formulation respectively.
- 318 • The flexural strength of the mass fraction equal to 12; 14; 16; 18; 20% and 25 of the PMxSed50 formulation
319 decreases by 53.88; 26.41; 41.58; 47.24; 33.77 and 22.97% compared to the PMxSed30 formulation
320 respectively.

321 Several factors affect flexural strength, such as the amount of resin, the nature and amount of the filler and the
322 particle size of the filler. In a research article [58], they arrived at the same results. The flexural strength of the
323 polymer mortars PMx and PMxSed30, PMxSed50 can be related to the mass percentage of the resin by a linear
324 relationship of positive slope with a correlation of 0.76 and 0.92, 0.92 respectively.

325 ***III.4. Modules of elasticity***

326 The figure 10 shows the modulus of elasticity of the mortars PMx, PMxSed30 and PMxSed50 as a function of the
327 mass fractions. The modulus of elasticity of the PMx mortar decreased by 10.05% for mass fraction between the
328 ranges of 16% to 25% there is an increase of 29.49% for mass fraction between 12% and 18%. It is observed that the
329 modulus of elasticity of the PMxSed50 formulation is increased from 1.45 GPa to 11.9 GPa when the mass fraction
330 increases from 12% to 25%. For the equal mass fraction 20, the modulus of elasticity of the mortar PMxSed30
331 slightly exceeds the modulus of elasticity of the PMx mortar. The modulus of elasticity of the mortar polymer
332 PMxSed30 is higher than that of the modulus of elasticity of the mortar PMxSed50, the difference percentages is
333 64.63; 34.21; 60.52; 48.54; 32.86 and 6.66 for the equal weight fraction 12; 14; 16; 18; 20 and 25% respectively.

334 It is observed that the modulus of elasticity is related to the mass fraction of the resin, the modulus of elasticity can
335 be related to the mass fraction of the binder with a linear function of the positive slope with a strong correlation of
336 0.79 and 0.97 for PMxSed30 and PMxSed50 formulations respectively. For the PMx formulation have a low

337 correlation of 0.10. It is concluded that the modulus of elasticity of the polymer mortar PMxSed30 and PMxSed50
338 increases when the quantity of the resin increases unlike the mortar PM it reaches the optimum value (the mass
339 fraction equal to 16%). The amount of sediment increases the modulus of elasticity decreases. This phenomenon can
340 be explained by the particle size of the sediment that affects the charge distribution in the matrix. The nature of the
341 sediment being different from that of sand, this difference influences the modulus of elasticity, which confirms in the
342 literature [59,60]. The interfacial load / matrix has an important role on the modulus of elasticity [61]. The bond of
343 the sand with the resin is different from the bonding of the sediment with the resin the adhesion force corresponds to
344 the chemical reactions between the load and the resin which this reaction depends on the elements that make up the
345 load.

346 *III.5. Porosity*

347 The figure (11 a) shows the porosity of the mortar PMx, PMxSed30 and PMxSed50 as a function of the mass
348 fraction. the value of the porosity of epoxy resin without charge is equal to 3.95% this porosity can be related to the
349 binder preparation, during the mixing air balls were observed where it can be related to the pressure exerted by the
350 mercury porosimetry on the composite. Note that the porosity of the PMx mortar decreases when the mass fraction of
351 the resin increases from 12% to 14%, the porosity increases by 68.43% when the mass fraction increases from 14%
352 to 25%, the same phenomenon observed in the study [33]. This phenomenon can be explained by the study of [62],
353 the fact that the apparent absorption of mercury by the polymer mortar fills the void in the material produced by the
354 collapse or compression of the material and that the material has a restitution or elasticity and resumes its original
355 shape or volume. But it is observed that 100% of the resin content that the porosity lower than the porosity of the
356 polymer mortar, can explain this difference by the fact that the mercury pressure applied to the charges leads to
357 applying a force on the matrix, which implies a deformation on the opens the pores.

358 The PMxSed30 mortar porosity value decreased by 80.38% when the resin mass fraction ranging from 12% to 18%,
359 and increases of 25.67%, when the resin mass fraction range from 18% to 25%. It is noted that the value of the
360 porosity of the mortar PMxSed50 is increased by 10.6% between the mass fraction of 12% to 14%, after the mass
361 fraction of 14%, the porosity decreases with a percentage of 71, 43%. The porosity of the PMxSed30 and PMxSed50
362 mortars related to the mass fraction by a relationship of negative slope. With regard to the PMx mortar, the porosity
363 can be related to the mass fraction by a linear relationship of positive slope with a correlation equal to 0.88. The
364 value of the porosity of the mortar PMx is large compared to the value of the porosity of binder; it is observed that
365 the percentage difference in value of the porosity between the mortar PMx and the binder increases with the increase
366 of the mass fraction. Contrary for the mortar PMxSed30 and PMxSed50 the value of the porosity becomes close to
367 the value of the porosity of binder with the increase of the mass fraction.

368 It is noted that over the mass fraction range of 12% to 25% the value of the porosity of the mortar PMxSed50 is
369 greater compared to the mortar PMxSed30. This difference can be explained by the amount of sediment increases
370 implies that the adhesion force between the load and the matrix is low; this weakness leads to empty spaces.

371 Sediments characterizations have a role on the porosity, the percentage of water absorption of the sediment is
372 important which leads to the absorption of the resin by the sediment until saturation.

373 The figure (11-b) shows the curve of the compressive strength as a function of the porosity. Note that the
374 compressive strength of the mortar PMxSed30 and PMxSed50 decreases when the porosity increases which is
375 equivalent to a decrease in the mass fraction of the binder. But the compressive strength of the mortar PMx is not
376 related to the porosity so that a weak correlation of 0.07. The compressive strength of the mortar PMxSed30 and
377 PMxSed50 can be related to the porosity by a linear relationship of negative slope with a correlation of 0.88 and
378 0.79, respectively.

379 **III.6. Water absorption**

380 Figure (12-a) illustrates the evolution of water absorption of the PMx mortar with different mass fractions of the
381 binder as a function of time. It should be noted that PMx water absorption decreases as the mass fraction of the
382 binder decreases. It should be noted that the PMx mortars are saturated from 4 hours except the PM12 mortar. Figure
383 (12-b) illustrates the evolution of the water absorption of the PMxSed30 mortar with different mass fractions as a
384 function of time. It should be noted that the water absorption of PMxSed30 decreases as the mass fraction of the
385 binder decreases. Mortars PM12Sed30, PM14Sed30 and PM16Sed30 saturate after 12 hours, unlike mortars
386 PM18Sed30, PM20Sed30 and PM25Sed30. The figure (12-c) illustrates the evolution of the water absorption of the
387 mortar PMxSed50 with different resin mass fractions as a function of time. It noted that the water absorption of
388 PMxSed30 decreases as the mass fraction of the binder decreases. PM12Sed50, PM14Sed50 and PM16Sed50
389 mortars saturate them from 12 hours unlike PM18Sed50, PM20Sed50 and PM25Sed50 mortars. Water absorption
390 increases as the percentage of sediment increases and the mass fraction of the binder decreases. In the literature [63]
391 they confirmed the relationship between resin quantity and water absorption. The resin covering the charges prevents
392 the penetration of water; when the amount of resin is insufficient to cover the entire charge the water penetrates
393 remains stuck in the mortar where the charges of the unsaturated sediment absorb it.

394 **III.7. Linear thermal expansion**

395 The figure 13 shows the evolution of the coefficient thermal expansion of the PMx, PMxSed30 and PMxSed50
396 mortars as a function of the mass fractions, we observe that:

- 397 • The graph of the thermal expansion of the PMx mortar is an increasing curve, the thermal expansion
398 increases as the mass fraction increases. The value of the thermal expansion is increased by a percentage of
399 33.33%; 37.49%; 38.7%; 18.6%; between the mass fraction of 12% to 14%; 14% to 16%; 18% to 20% and
400 20% to 25% respectively and a slight decrease of 6.06% between the mass fraction of 16% to 18%. The
401 thermal expansion curve of the PMx mortar can be connected to the mass fraction by a linear relationship of
402 positive slope with a correlation of 0.94.
- 403 • The thermal expansion curve of the PMxSed30 mortar is an increasing curve as a function of the mass
404 fractions. It is observed that between the intervals of the mass fraction comprised between 12% to 14%;

405 16% to 18%; 18% to 20% and 20% to 25%, the value of thermal expansion increases by a percentage of
406 36.36; 78.57; 27.99 and 21.87 respectively. For the interval between 14% and 16%, the value of the thermal
407 expansion reduces by 6.66%. The thermal expansion curve of the PMxSed30 mortar can be related to the
408 mass fraction by a linear relationship of positive slope with a correlation of 0.93

- 409 • The thermal expansion curve of the mortar PMxSed50 is increasing as a function of the mass fraction of the
410 binder, it is found that the value of the thermal expansion increases by a percentage of 175; 63.63; 27.77
411 and 17.39% between the mass fractions of 14% to 16%; 16% to 18%; 18% to 20% and 20% to 25%
412 respectively. Between the mass fractions of 12% to 14% decreases by 20%. The thermal expansion curve of
413 the PMxSed50 mortar can be connected to the mass fraction by a linear relationship of positive slope with a
414 correlation of 0.91

415 The coefficient of thermal expansion of epoxy mortars is higher; the thermal expansion coefficient increases as the
416 amount of resin increases and the coefficient of thermal expansion decreases when the load increases even remarks
417 reported in a paper search [64]. These results can be explained by the connection between the charge and the matrix;
418 when the important bond the coefficient thermal expansion is high. the type and shape of the load influences the
419 thermal expansion coefficient we note that the thermal dilation coefficient of PMx is different from PMxSedy, in the
420 literature have shown that the nature of charge [65] and the shape [66].

421 ***III.8. The thermal shock resistance***

422 From visual examination according to the conditions of the standard on a surface treated with methyl blue, the
423 modifications observed are small cracks and exfoliations on PM12Sed30 and PM12Sed50 formulations; these
424 modifications can be explained by the low resin content which leads to a weak bond between the fillers and the
425 matrix; for other formulations no modification. In a paper search [31], they did not observe modifications for a
426 polymer mortar with a mass fraction of 30% epoxy and 70% of fillers (crushed granite).

427 ***III.9. Chemical resistance***

428 It was noticed that the PM12 Sed30 and PM12 Sed50 and PM14 Sed50 formulations are not resistant to the attacks
429 of the solutions (KOH and HCl). Modifications have been observed on the surface of the tested samples and that the
430 solutions attack the load, these attacks related to the small amount of resin that covers the charges. In the researches
431 [68] have tested several chemical solutions on epoxy mortars. They concluded that epoxy mortars are resistant to
432 chemical attack.

433 ***III.10. Leaching test of crushed samples***

434 The **table 6** shows the results of the leaching of the PMxSed30 mortar of the different mass fractions of binder. It is
435 noted that for PMxSed30 mortar of different mass fraction the leaching result shows that the value of the antimony
436 element (Sb) is exceeded the threshold. The soluble fraction value of the mortar PM18Sed30, PM20Sed30 and
437 PM25Sed30 exceeds the threshold. It should be noted that the values of the chemical elements of the PMxSed30

438 mortar are less than or equal to the values of the raw sediment. The fluoride value of the raw sediment is exceeded
439 the threshold but after the incorporation of the sediment in a polymer matrix this value has decreased and the more
440 the mass fraction of the binder increases this value decreases. The pH of the PMxSed30 mortar is almost stable and
441 its value between the pH value of the sediment and the value of the sand. The soluble fraction increases with the
442 increase of the mass fraction of the binder. The conductivity of the PMxSed30 mortar is small compared to the raw
443 sediment but it is large compared to the sand. The PMxSed30 mortar of the different mass fraction of the binder is a
444 non-inert and non-hazardous mortar. The **table 7** shows the results of the leaching of the PMxSed50 mortar of the
445 different mass fractions of binder. It is noted that for **PMxSed30** mortar of different mass fraction the leaching result
446 shows that the value of the antimony element (Sb) is exceeded the threshold. The value of the soluble fraction of
447 PMxSed50 mortar for all mass fractions of binder exceeds the thresholds. It should be noted that PMxSed50 mortar
448 chemical values are less than or equal to raw sediment values. The fluoride value of the raw sediment is exceeded,
449 but after the incorporation of the sediment in a polymer matrix, this value has decreased except for the PM12Sed50
450 mortar where the amount of binder is low, the fluoride value decreases when the quantity of resin increases.

451 The pH of the PMxSed50 mortar is almost stable and its value between the pH value of the sediment and the value of
452 the sand. The soluble fraction increases with the increase of the mass fraction of the binder. The conductivity of the
453 PMxSed50 mortar is small compared to the raw sediment but it is large compared to the sand. The PMxSed50 mortar
454 of the different mass fraction of the binder is a non-inert and non-hazardous mortar. The explanation of the decrease
455 in the chemical values of the raw sediment after the incorporation of the sediments in a polymer matrix, the sediment
456 loads are covered by the binder which prevents the diffusion of the chemical elements in the solution. Mainly, the
457 increase of the soluble fraction is bound to the resin.

458 ***III.11. SEM observation***

459 Scanning electron microscopy (SEM) of hardened polymer mortar was performed and observations were made on
460 the different formulations to investigate the sediment effect on the interface microstructure. The scanning electron
461 microscope (SEM) analysis shows the good bonds between aggregates and epoxy resin. Hardened polymer mortar
462 observation shows a good dense and consistent structure, which is in agreement of previous study [69]. Otherwise it
463 can observe that the porosity in the composite is clearly influenced by the replacement of sand by sediment and the
464 amount of epoxy resin/sediment in the matrices. This may also be due to the chemicals elements that make up the
465 material in the sediments.

466 **IV. Conclusion and perspectives**

467 This research paper has shown the feasibility of optimizing sediments in a polymer matrix with the packing density
468 model I, this model can give approximate percentages of the constituents to obtain an optimal compactness of the
469 mixture; the porosity of the mixture given by the model may be the approximate amount of binder to be added.

470 The curing time of the polymer mortar made by sediments is identical to that of the polymer mortar made by sand.
471 Tests of flexural, compressive strength and modulus of elasticity have shown good results, mechanical properties are

472 related to the amount of resin and the nature of sediments. From the determined mass fraction of the binder, the
473 results of the mechanical tests of the polymer mortar made by sediment exceed the results of the mechanical tests of
474 a polymer mortar made by standardized sand. The mechanical properties can be improved if the sediment is saturated
475 with a solution that does not react with the resin or with a surface treatment of the sediment to increase the adhesion
476 forces between the sediment and the matrix.

477 The polymer mortar made by sediment has good physical properties. Mercury porosity and water absorption are
478 related to the amount of resin and the amount of sediment. There is a linear relationship between compressive
479 strength and porosity for polymer mortar made with sediment unlike mortar made with sand. The water absorption of
480 the polymer mortar made by sand is low compared to the polymer mortar made by sediment, this difference related
481 to the high water content of the sediment.

482 The polymer mortar made by sediment showed good thermal properties when compared to the polymer mortar made
483 by sand, the incorporation of the sediment in a polymer matrix has influenced the thermal properties. The polymer
484 mortar made by sediment has shown good durability to chemical attack and thermal shock, the durability of the
485 polymer mortar manufactured by sediment is related to the nature and quantity of the load and the amount of binder.
486 The leaching test has shown that the epoxy resin has an important role of covering the load, this cover limits the
487 diffusion of the chemical elements.

488 **Acknowledgements:** This project was initiated in the Haut de France Region (France), collaboration IMT LILLE
489 DOUAI and Neo Eco Recycling. The authors thank the European Regional Development Fund (ERDF) for their
490 financial support to the project.

491 **Reference**

492 [1] P.-Y. Scordia, Caractérisation et valorisation de sédiments fluviaux pollués et traités dans les
493 matériaux routiers, (n.d.) 203.

494 [2] E. Rozière, M. Samara, A. Loukili, D. Damidot, Valorisation of sediments in self-consolidating
495 concrete: Mix-design and microstructure, *Construction and Building Materials*. 81 (2015) 1–10.
496 doi:10.1016/j.conbuildmat.2015.01.080.

497 [3] M. Benzerzour, Y. Mamindy-Pajany, E. van Veen, M. Boutouil, N.E. Abriak, Beneficial reuse of
498 Brest-Harbor (France)-dredged sediment as alternative material in road building: laboratory
499 investigations, *Environmental Technology*. 39 (2018) 566–580. doi:10.1080/09593330.2017.1308440.

500 [4] F. Hamouche, R. Zentar, Effects of Organic Matter on Physical Properties of Dredged Marine
501 Sediments, *Waste and Biomass Valorization*. (2018). doi:10.1007/s12649-018-0387-6.

502 [5] N. Junakova, J. Junak, M. Balintova, Reservoir sediment as a secondary raw material in concrete
503 production, *Clean Technologies and Environmental Policy*. 17 (2015) 1161–1169. doi:10.1007/s10098-
504 015-0943-8.

- 505 [6] K. Siham, B. Fabrice, A.N. Edine, D. Patrick, Marine dredged sediments as new materials resource
506 for road construction, *Waste Management*. 28 (2008) 919–928. doi:10.1016/j.wasman.2007.03.027.
- 507 [7] V. Dubois, N.E. Abriak, R. Zentar, G. Ballivy, The use of marine sediments as a pavement base
508 material, *Waste Management*. 29 (2009) 774–782. doi:10.1016/j.wasman.2008.05.004.
- 509 [8] R. Zentar, D. Wang, N.E. Abriak, M. Benzerzour, W. Chen, Utilization of siliceous–aluminous fly
510 ash and cement for solidification of marine sediments, *Construction and Building Materials*. 35 (2012)
511 856–863. doi:10.1016/j.conbuildmat.2012.04.024.
- 512 [9] M. Amar, M. Benzerzour, A.E.M. Safhi, N.-E. Abriak, Durability of a cementitious matrix based on
513 treated sediments, *Case Studies in Construction Materials*. 8 (2018) 258–276.
514 doi:10.1016/j.cscm.2018.01.007.
- 515 [10] J. Couvidat, M. Benzaazoua, V. Chatain, A. Bouamrane, H. Bouzahzah, Feasibility of the reuse of
516 total and processed contaminated marine sediments as fine aggregates in cemented mortars,
517 *Construction and Building Materials*. 112 (2016) 892–902. doi:10.1016/j.conbuildmat.2016.02.186.
- 518 [11] A. el M. Safhi, M. Benzerzour, P. Rivard, N.-E. Abriak, I. Ennahal, Development of self-compacting
519 mortars based on treated marine sediments, *Journal of Building Engineering*. 22 (2019) 252–261.
520 doi:10.1016/j.jobbe.2018.12.024.
- 521 [12] C.-L. Hwang, L.A.-T. Bui, K.-L. Lin, C.-T. Lo, Manufacture and performance of lightweight
522 aggregate from municipal solid waste incinerator fly ash and reservoir sediment for self-consolidating
523 lightweight concrete, *Cement and Concrete Composites*. 34 (2012) 1159–1166.
524 doi:10.1016/j.cemconcomp.2012.07.004.
- 525 [13] C.-W. Tang, H.-J. Chen, S.-Y. Wang, J. Spaulding, Production of synthetic lightweight aggregate
526 using reservoir sediments for concrete and masonry, *Cement and Concrete Composites*. 33 (2011) 292–
527 300. doi:10.1016/j.cemconcomp.2010.10.008.
- 528 [14] M. BENKADDOUR, F.K. AOUAL, A. SEMCHA, Durabilité des mortiers à base de pouzzolane
529 naturelle et de pouzzolane artificielle, (n.d.) 11.
- 530 [15] A. el Mahdi Safhi, M. Benzerzour, P. Rivard, N.-E. Abriak, Feasibility of using marine sediments in
531 SCC pastes as supplementary cementitious materials, *Powder Technology*. 344 (2019) 730–740.
532 doi:10.1016/j.powtec.2018.12.060.
- 533 [16] A.L.G. Gastaldini, M.P. da Silva, F.B. Zamberlan, C.Z. Mostardeiro Neto, Total shrinkage, chloride
534 penetration, and compressive strength of concretes that contain clear-colored rice husk ash,
535 *Construction and Building Materials*. 54 (2014) 369–377. doi:10.1016/j.conbuildmat.2013.12.044.
- 536 [17] A. Tironi, M.A. Trezza, A.N. Scian, E.F. Irassar, Assessment of pozzolanic activity of different
537 calcined clays, *Cement and Concrete Composites*. 37 (2013) 319–327.
538 doi:10.1016/j.cemconcomp.2013.01.002.

- 539 [18] M. Jamshidi, A.R. Pourkhorshidi, Modified polyester resins as an effective binder for polymer
540 concretes, *Materials and Structures*. 45 (2012) 521–527. doi:10.1617/s11527-011-9779-9.
- 541 [19] J.I. Daniel, V.S. Gopalaratnam, M.A. Galinat, Reported by ACI Committee 544, (n.d.) 66.
- 542 [20] J.M.. Reis, A.J.. Ferreira, Assessment of fracture properties of epoxy polymer concrete reinforced
543 with short carbon and glass fibers, *Construction and Building Materials*. 18 (2004) 523–528.
544 doi:10.1016/j.conbuildmat.2004.04.010.
- 545 [21] W. Lokuge, T. Aravinthan, Effect of fly ash on the behaviour of polymer concrete with different
546 types of resin, *Materials & Design*. 51 (2013) 175–181. doi:10.1016/j.matdes.2013.03.078.
- 547 [22] J.P. Gorninski, D.C. Dal Molin, C.S. Kazmierczak, Comparative assessment of isophthalic and
548 orthophthalic polyester polymer concrete: Different costs, similar mechanical properties and durability,
549 *Construction and Building Materials*. 21 (2007) 546–555. doi:10.1016/j.conbuildmat.2005.09.003.
- 550 [23] Rebeiz K. S., Craft A. P., Polymer Concrete Using Coal Fly Ash, *Journal of Energy Engineering*. 128
551 (2002) 62–73. doi:10.1061/(ASCE)0733-9402(2002)128:3(62).
- 552 [24] M.J. Hashemi, M. Jamshidi, Flexural Behavior of Polyester Polymer Concrete Subject to Different
553 Chemicals, 28 (2015) 7.
- 554 [25] E. Ghorbel, M. Haidar, Durability to Chemical Attack by Acids of Epoxy Microconcretes by
555 Comparison to Cementitious Ones, *Advances in Civil Engineering*. 2016 (2016) 1–15.
556 doi:10.1155/2016/4728372.
- 557 [26] C. Vipulanandan, N. Dharmarajan, Flexural behavior of polyester polymer concrete, *Cement and
558 Concrete Research*. 17 (1987) 219–230. doi:10.1016/0008-8846(87)90105-0.
- 559 [27] H. Abdel-Fattah, M.M. El-Hawary, Flexural behavior of polymer concrete, *Construction and
560 Building Materials*. 13 (1999) 253–262. doi:10.1016/S0950-0618(99)00030-6.
- 561 [28] M. Muthukumar, D. Mohan, Studies on polymer concretes based on optimized aggregate mix
562 proportion, *European Polymer Journal*. 40 (2004) 2167–2177. doi:10.1016/j.eurpolymj.2004.05.004.
- 563 [29] K.C. Radford, The mechanical properties of an epoxy resin with a second phase dispersion,
564 *Journal of Materials Science*. 6 (1971) 1286–1291. doi:10.1007/bf00552042.
- 565 [30] Y. Nakamura, M. Yamaguchi, M. Okubo, T. Matsumoto, Effects of particle size on mechanical and
566 impact properties of epoxy resin filled with spherical silica, *Journal of Applied Polymer Science*. 45 (1992)
567 1281–1289. doi:10.1002/app.1992.070450716.
- 568 [31] A.T. Dibenedetto, A.D. Wambach, The Fracture Toughness of Epoxy-glass Bead Composites,
569 *International Journal of Polymeric Materials*. 1 (1972) 159–173. doi:10.1080/00914037208082114.
- 570 [32] J.M.L. Reis, Fracture and flexural characterization of natural fiber-reinforced polymer concrete,
571 *Construction and Building Materials*. 20 (2006) 673–678. doi:10.1016/j.conbuildmat.2005.02.008.

- 572 [33] H.G. Nguyen, S. Ortola, E. Ghorbel, Micromechanical modelling of the elastic behaviour of
573 polymer mortars, *European Journal of Environmental and Civil Engineering*. 17 (2013) 65–83.
574 doi:10.1080/19648189.2012.739787.
- 575 [34] M. Hassani Niaki, A. Fereidoon, M. Ghorbanzadeh Ahangari, a novel, *Structural Concrete*. 19
576 (2018) 366–373. doi:10.1002/suco.201700003.
- 577 [35] S.-C. Kou, C.-S. Poon, A novel polymer concrete made with recycled glass aggregates, fly ash and
578 metakaolin, *Construction and Building Materials*. 41 (2013) 146–151.
579 doi:10.1016/j.conbuildmat.2012.11.083.
- 580 [36] Comparison of Mechanical Properties for Polymer Concrete with Different Types of Filler |
581 *Journal of Materials in Civil Engineering* | Vol 22, No 7, (n.d.).
582 [https://ascelibrary.org/doi/abs/10.1061/\(ASCE\)MT.1943-5533.0000069](https://ascelibrary.org/doi/abs/10.1061/(ASCE)MT.1943-5533.0000069) (accessed November 2, 2018).
- 583 [37] K.S. Rebeiz, S.P. Serhal, A.P. Craft, Properties of Polymer Concrete Using Fly Ash, *Journal of*
584 *Materials in Civil Engineering*. 16 (2004) 15–19. doi:10.1061/(ASCE)0899-1561(2004)16:1(15).
- 585 [38] A. Kumar, G. Singh, N. Bala, Evaluation of Flexural Strength of Epoxy Polymer Concrete with Red
586 Mud and Fly Ash, *International Journal of Current Engineering and Technology*. (2013) 5.
- 587 [39] J.M.L. Reis, R. Chianelli-Junior, J.L. Cardoso, F.J.V. Marinho, Effect of recycled PET in the fracture
588 mechanics of polymer mortar, *Construction and Building Materials*. 25 (2011) 2799–2804.
589 doi:10.1016/j.conbuildmat.2010.12.056.
- 590 [40] G. Sosoi, M. Barbuta, A.A. Serbanoiu, D. Babor, A. Burlacu, Wastes as aggregate substitution in
591 polymer concrete, *Procedia Manufacturing*. 22 (2018) 347–351. doi:10.1016/j.promfg.2018.03.052.
- 592 [41] N. Benzannache, A. Bezazi, H. Bouchelaghem, M. Boumaaza, S. Amziane, F. Scarpa, Statistical
593 Analysis of 3-Point Bending Properties of Polymer Concretes Made From Marble Powder Waste, Sand
594 Grains, and Polyester Resin, *Mechanics of Composite Materials*. 53 (2018) 781–790. doi:10.1007/s11029-
595 018-9703-2.
- 596 [42] N.E. Marcovich, M.M. Reboledo, M.I. Aranguren, Mechanical properties of woodflour
597 unsaturated polyester composites, *Journal of Applied Polymer Science*. 70 (1998) 2121–2131.
598 doi:10.1002/(SICI)1097-4628(19981212)70:11<2121::AID-APP5>3.0.CO;2-Z.
- 599 [43] I. Ennahal, W. Maherzi, Y. Mamindy-Pajany, M. Benzerzour, N.-E. Abriak, Eco-friendly polymers
600 mortar for floor covering based on dredged sediments of the north of France, *Journal of Material Cycles*
601 *and Waste Management*. (2019). doi:10.1007/s10163-019-00843-3.
- 602 [44] A. Lecomte, J.-M. Mechling, C. Diliberto, Compaction index of cement paste of normal
603 consistency, *Construction and Building Materials*. 23 (2009) 3279–3286.
604 doi:10.1016/j.conbuildmat.2009.05.005.

- 605 [45] Essai de compacité des fractions granulaires à la table à secousses: mode opératoire.,
606 Laboratoire central des ponts et chaussées, Paris, 2004.
- 607 [46] Elalaoui et al. - 2012 - Mechanical and physical properties of epoxy polymers.pdf, (n.d.).
608 [https://ac.els-cdn.com/S0950061811003813/1-s2.0-S0950061811003813-main.pdf?_tid=033ade1e-](https://ac.els-cdn.com/S0950061811003813/1-s2.0-S0950061811003813-main.pdf?_tid=033ade1e-482e-4ff2-b73d-a8c19960694f&acdnat=1535617709_40b87b5917863fa5655d02eab6da5bab)
609 [482e-4ff2-b73d-a8c19960694f&acdnat=1535617709_40b87b5917863fa5655d02eab6da5bab](https://ac.els-cdn.com/S0950061811003813/1-s2.0-S0950061811003813-main.pdf?_tid=033ade1e-482e-4ff2-b73d-a8c19960694f&acdnat=1535617709_40b87b5917863fa5655d02eab6da5bab) (accessed
610 August 30, 2018).
- 611 [47] P.J.R.O. Nóvoa, M.C.S. Ribeiro, A.J.M. Ferreira, Mechanical Behaviour of Cork-Modified Polymer
612 Concrete, *Materials Science Forum*. 455–456 (2004) 805–809. doi:10.4028/www.scientific.net/MSF.455-
613 456.805.
- 614 [48] Y. Ohama, K. Demura, Relation between curing conditions and compressive strength of polyester
615 resin concrete, *International Journal of Cement Composites and Lightweight Concrete*. 4 (1982) 241–244.
616 doi:10.1016/0262-5075(82)90028-8.
- 617 [49] M.E. Tawfik, S.B. Eskander, Polymer Concrete from Marble Wastes and Recycled Poly(ethylene
618 terephthalate), *Journal of Elastomers & Plastics*. 38 (2006) 65–79. doi:10.1177/0095244306055569.
- 619 [50] K.S. Rebeiz, Precast use of polymer concrete using unsaturated polyester resin based on recycled
620 PET waste, *Construction and Building Materials*. 10 (1996) 215–220. doi:10.1016/0950-0618(95)00088-7.
- 621 [51] D.M. Yemam, B.-J. Kim, J.-Y. Moon, C. Yi, Mechanical Properties of Epoxy Resin Mortar with Sand
622 Washing Waste as Filler, *Materials (Basel)*. 10 (2017). doi:10.3390/ma10030246.
- 623 [52] C. Vipulanandan, N. Dharmarajan, Flexural behavior of polyester polymer concrete, *Cement and*
624 *Concrete Research*. 17 (1987) 219–230. doi:10.1016/0008-8846(87)90105-0.
- 625 [53] S.-Y. Fu, X.-Q. Feng, B. Lauke, Y.-W. Mai, Effects of particle size, particle/matrix interface
626 adhesion and particle loading on mechanical properties of particulate–polymer composites, *Composites*
627 *Part B: Engineering*. 39 (2008) 933–961. doi:10.1016/j.compositesb.2008.01.002.
- 628 [54] M. Golestaneh, G. Amini, G.D. Najafpour, M.A. Beygi, Evaluation of mechanical strength of epoxy
629 polymer concrete with si, (2010) 6.
- 630 [55] P. Ravikumar, V. Ellappan, THE MIX PROPORTION AND STRENGTH OF POLYESTER RESIN
631 CONCRETE WITH VARIOUS MICROFILLERS, (n.d.) 9.
- 632 [56] A.J.M. Ferreira, C. Tavares, C. Ribeiro, Flexural Properties of Polyester Resin Concretes, *Journal of*
633 *Polymer Engineering*. 20 (2000). doi:10.1515/POLYENG.2000.20.6.459.
- 634 [57] M.C.S. Ribeiro, P.R. Nóvoa, A.J.M. Ferreira, A.T. Marques, Flexural performance of polyester and
635 epoxy polymer mortars under severe thermal conditions, *Cement and Concrete Composites*. 26 (2004)
636 803–809. doi:10.1016/S0958-9465(03)00162-8.

637 [58] M.C.S. Ribeiro, C.M.L. Tavares, M. Figueiredo, A.J.M. Ferreira, A.A. Fernandes, Bending
638 characteristics of resin concretes, *Materials Research*. 6 (2003) 247–254. doi:10.1590/s1516-
639 14392003000200021.

640 [59] Y. Nakamura, M. Yamaguchi, M. Okubo, T. Matsumoto, Effect of particle size on mechanical
641 properties of epoxy resin filled with angular-shaped silica, *Journal of Applied Polymer Science*. 44 (1992)
642 151–158. doi:10.1002/app.1992.070440116.

643 [60] X.L. Ji, J.K. Jing, W. Jiang, B.Z. Jiang, Tensile modulus of polymer nanocomposites, *Polymer*
644 *Engineering & Science*. 42 (2002) 983–993. doi:10.1002/pen.11007.

645 [61] Mechanical properties of particulate composites, *Composites*. 4 (1973) 93. doi:10.1016/0010-
646 4361(73)90794-5.

647 [62] P.A. Webb, *An Introduction To The Physical Characterization of Materials by Mercury Intrusion*
648 *Porosimetry with Emphasis On Reduction And Presentation of Experimental Data*, (n.d.) 23.

649 [63] M. Haidar, E. Ghorbel, H. Toutanji, Optimization of the formulation of micro-polymer concretes,
650 *Construction and Building Materials*. 25 (2011) 1632–1644. doi:10.1016/j.conbuildmat.2010.10.010.

651 [64] M.C.S. Ribeiro, J.M.L. Reis, A.J.M. Ferreira, A.T. Marques, Thermal expansion of epoxy and
652 polyester polymer mortars—plain mortars and fibre-reinforced mortars, *Polymer Testing*. 22 (2003) 849–
653 857. doi:10.1016/S0142-9418(03)00021-7.

654 [65] C.P. Wong, R.S. Bollampally, Thermal conductivity, elastic modulus, and coefficient of thermal
655 expansion of polymer composites filled with ceramic particles for electronic packaging, *Journal of*
656 *Applied Polymer Science*. 74 (1999) 3396–3403. doi:10.1002/(SICI)1097-
657 4628(19991227)74:14<3396::AID-APP13>3.0.CO;2-3.

658 [66] T.S. Chow, Effect of particle shape at finite concentration on thermal expansion of filled
659 polymers, *Journal of Polymer Science: Polymer Physics Edition*. 16 (1978) 967–970.
660 doi:10.1002/pol.1978.180160603.

661 [67] L. Agavriloaie, S. Oprea, M. Barbuta, F. Luca, Characterisation of polymer concrete with epoxy
662 polyurethane acryl matrix, *Construction and Building Materials*. 37 (2012) 190–196.
663 doi:10.1016/j.conbuildmat.2012.07.037.

664 [68] M. Golestaneh, Evaluation of Chemical Resistance of Polymer Concrete in Corrosive
665 Environments, *Iranica Journal of Energy & Environment*. 4 (2013). doi:10.5829/idosi.ijee.2013.04.03.19.

666 [69] Wang, Jiaqing, et al. "Mechanical and durability performance evaluation of crumb rubber-
667 modified epoxy polymer concrete overlays." *Construction and Building Materials* 203 (2019): 469-480.

668

Study of the polymer mortar based on dredged sediments and epoxy resin: Effect of the sediments on the behavior of the polymer mortar

Walid MAHERZI, Mahfoud BENZERZOUR, · Ilyas ENNAHAL, · Yannick MAMINDY-PAJANY, · Nor-Edine ABRIAK

LGCgE-Laboratoire de Génie Civil et géoEnvironnement, Département Génie Civil and Environnemental, IMT Lille-Douai, Univ. Lille, EA 4515, 764 BD Lahure, 59500 Douai, France

Figures

Figure 1. Navigable network of the Nord-Pas de Calais Regional Directorate of Voiesnavigables de France (VNF-SDRTD, 2009)	2
Figure 2. Particle size distribution of aggregates	2
Figure 3. Evolution of the packing density of the mixtures	3
Figure 4. (a) and (b) and (c) show the evolution of the density of PMx and PMxSed30, PMxSed50 respectively, as a function of curing age.	3
Figure 5. Comparison between different densities of mix at 28 days	4
Figure 6. (a) and (b), (c) show the evolution of the compressive strength of PMx and PMxSed30, PMxSed50 respectively, versus curing age	5
Figure 7. Compressive strength of PMx, PMxSed30 and PMxSed50 versus mass fraction	6
Figure 8. (a) and (b), (c) show the evolution of the flexural strength of PMx and PMxSed30, PMxSed50 respectively, versus curing age.....	6
Figure 9. Flexural strength of PMx, PMxSed30 and PMxSed50 versus mass fraction of resin	7
Figure 10. Modulus of elasticity of PMx, PMxSed30 and PMxSed50 versus mass fraction of resin.....	7
Figure 11. (a) Evolution of the porosity of the mortar PMx, PMxSed30 and PMxSed50 versus mass fraction ; (b) the compressive strength as a function of the porosity.....	8
Figure 12. (a), (b) and (c) the water absorption of the PMx and PMxSed30, PMxSed50 mortar respectively as a function of curing time.....	8
Figure 13. Evolution of the coefficient of thermal expansion of the PMx, PMxSed30 and PMxSed50.	9
Figure 14. Scanning electron microscope (SEM) photograph from fracture surface of different formulation.....	10



Figure 1. Navigable network of the Nord-Pas de Calais Regional Directorate of Voies navigables de France (VNF-SDRTD, 2009)

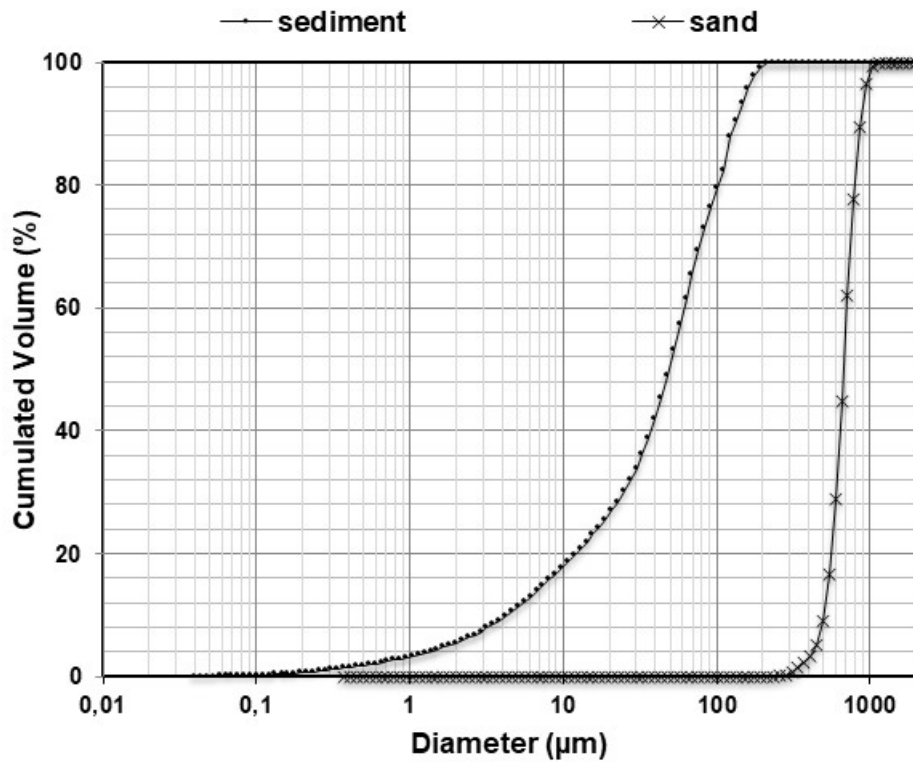


Figure 2. Particle size distribution of aggregates

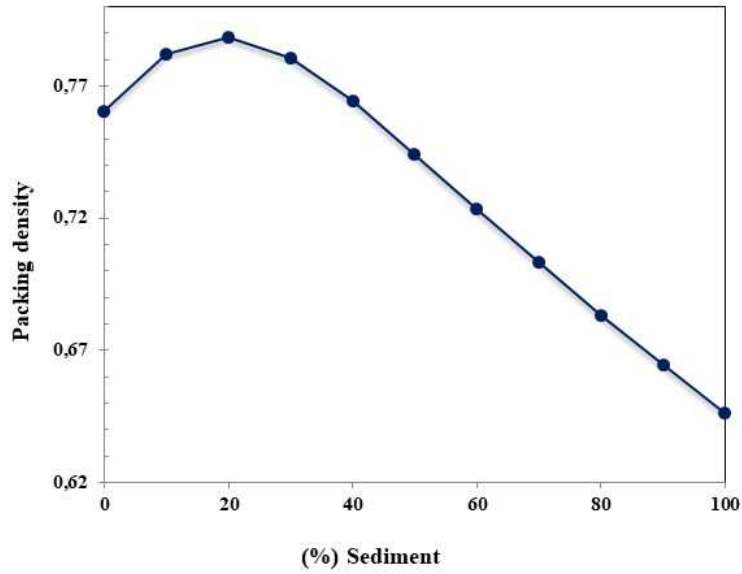


Figure 3. Evolution of the packing density of the mixtures

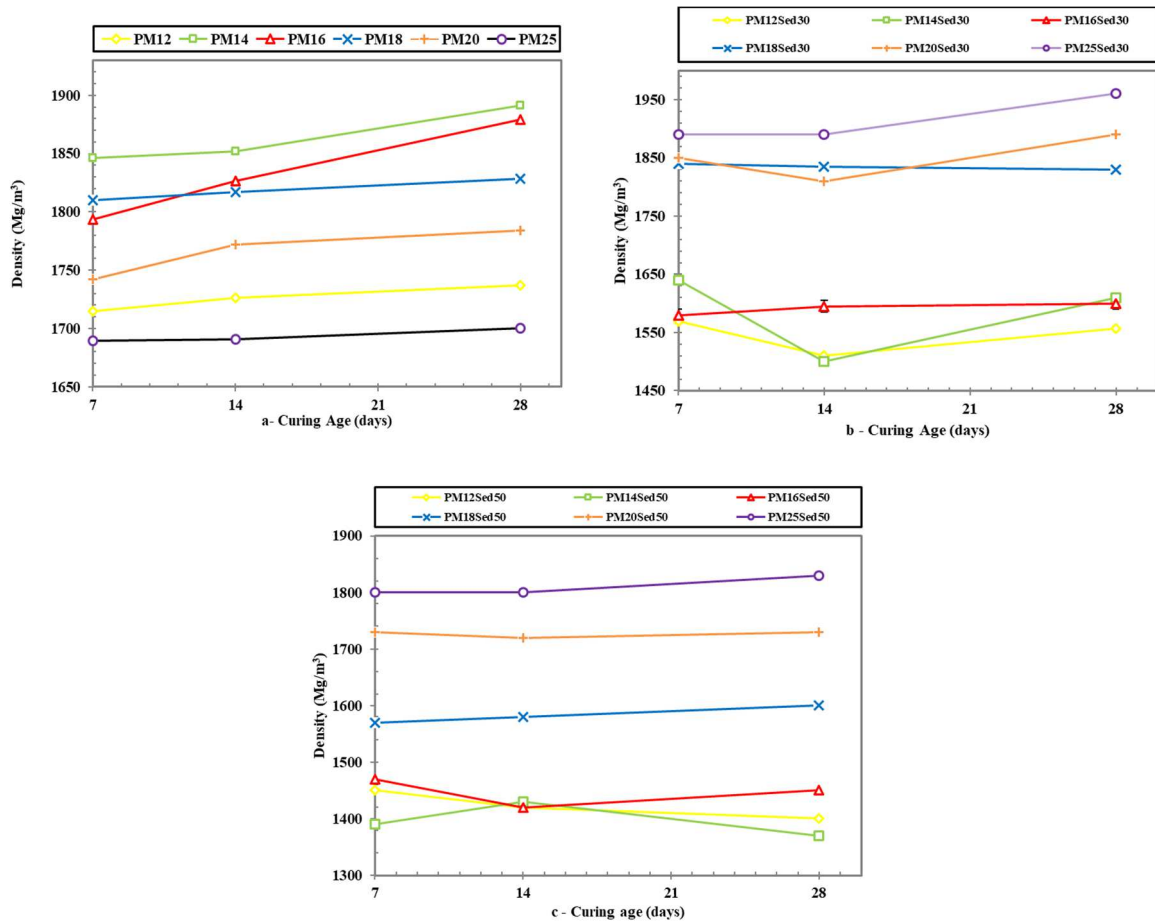


Figure 4. (a) (b) (c) evolution of the density of PMx and PMxSed30, PMxSed50 respectively, as a function of curing age.

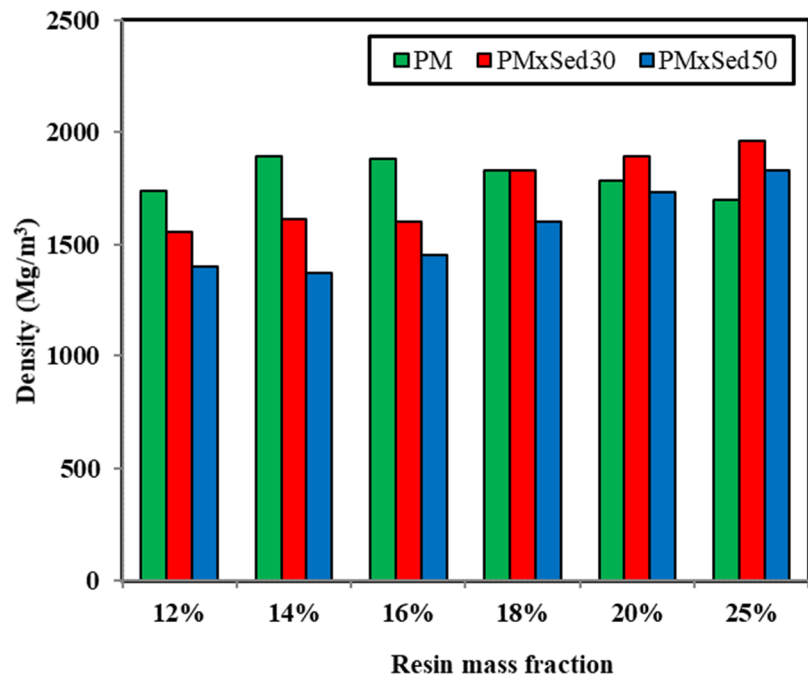


Figure 5. Comparison between different densities of mix at 28 days

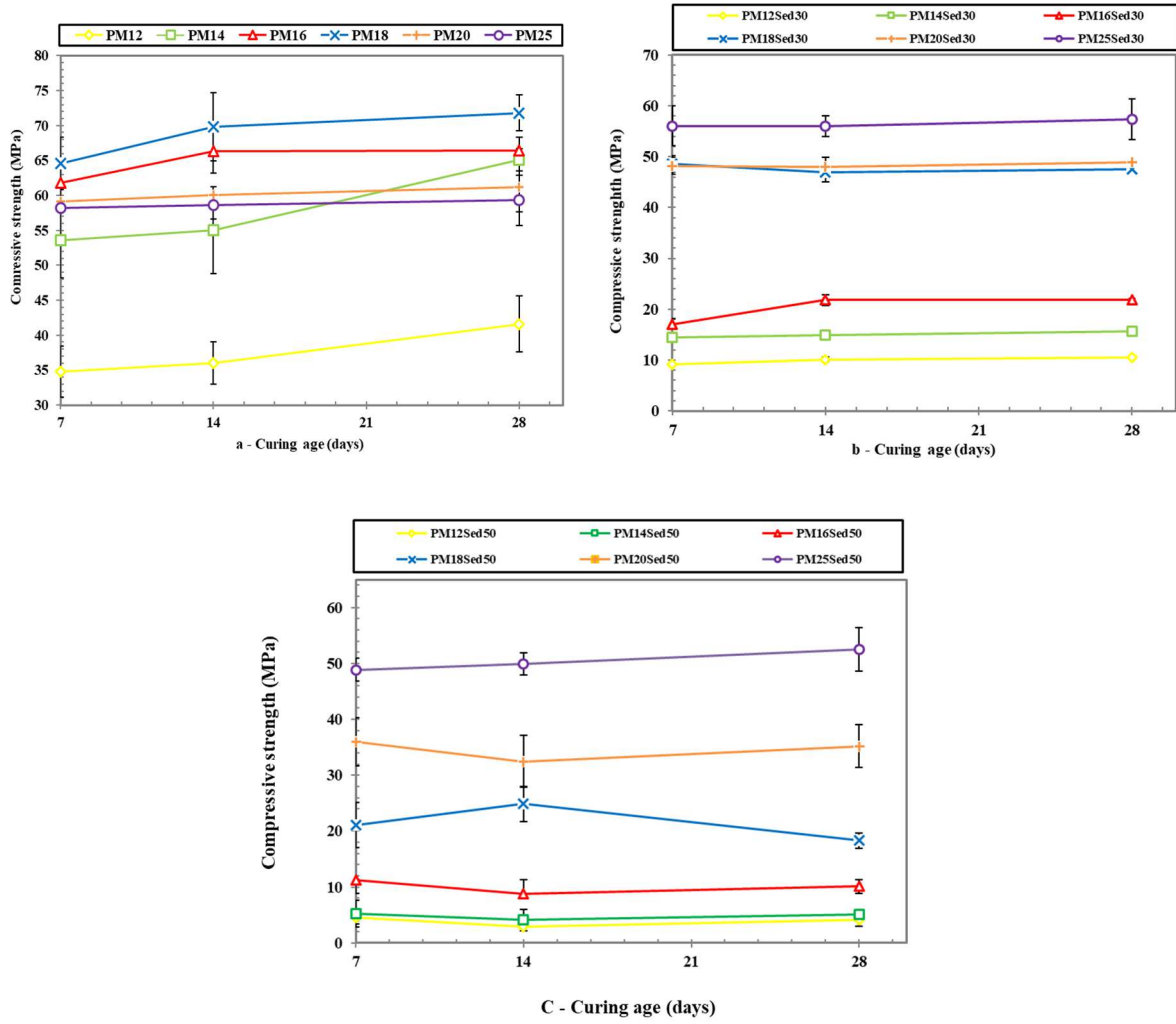


Figure 6. (a), (b), (c) show the evolution of the compressive strength of PMx and PMxSed30, PMxSed50 respectively, versus curing age

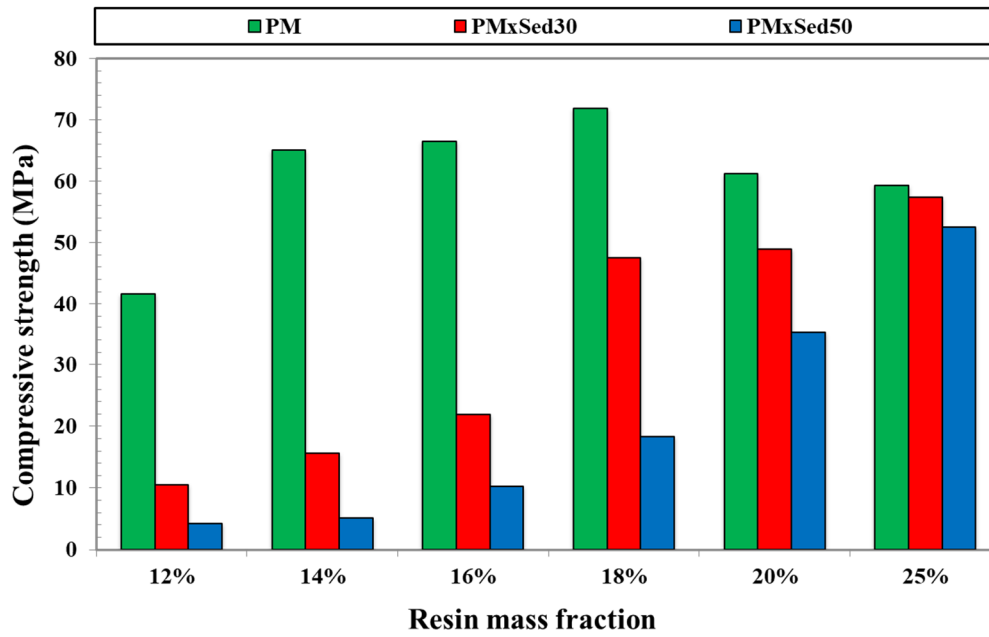


Figure 7. Compressive strength of PMx, PMxSed30 and PMxSed50 versus resin mass fraction

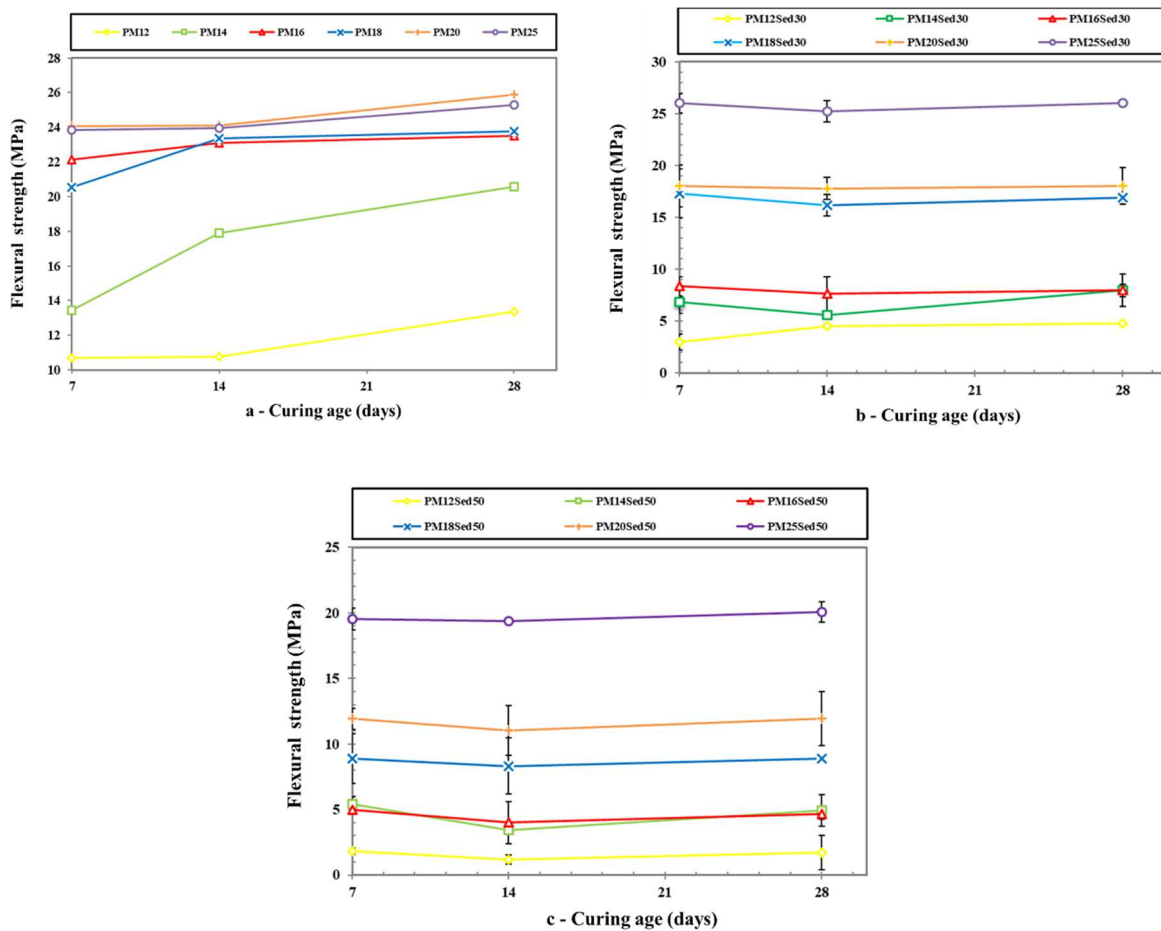


Figure 8. (a), (b), (c) show the evolution of the flexural strength of PMx and PMxSed30, PMxSed50 respectively, versus curing age

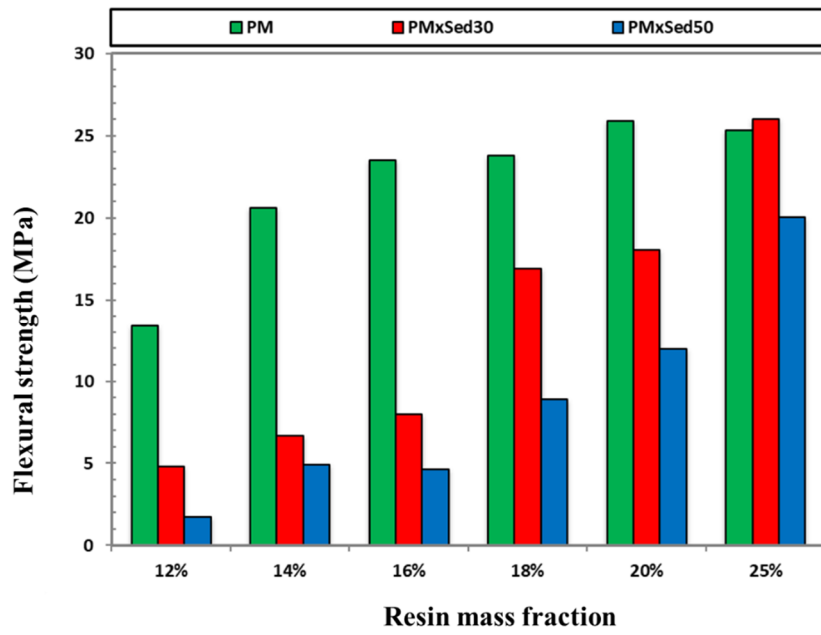


Figure 9. Flexural strength of PMx, PMxSed30 and PMxSed50 versus mass fraction of resin

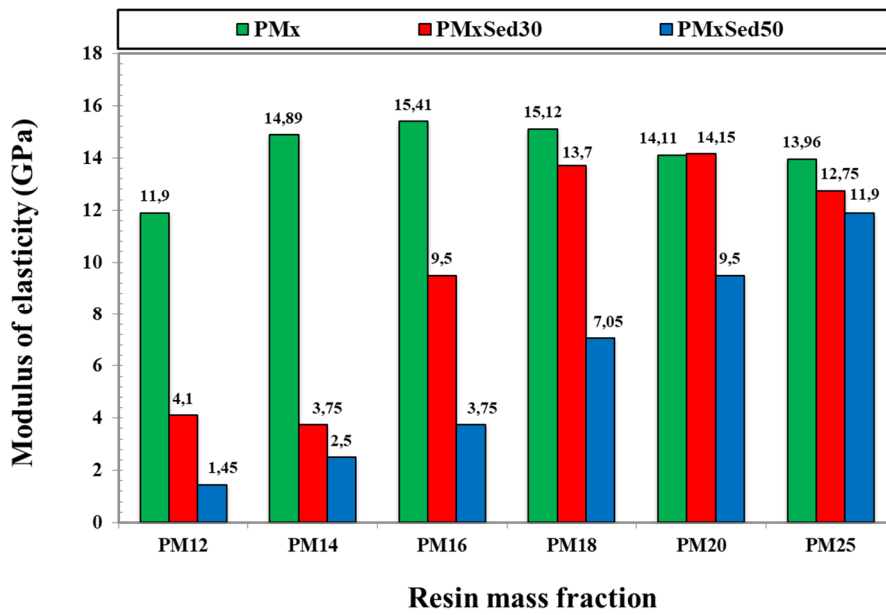


Figure 10. Modulus of elasticity of PMx, PMxSed30 and PMxSed50 versus mass fraction of resin

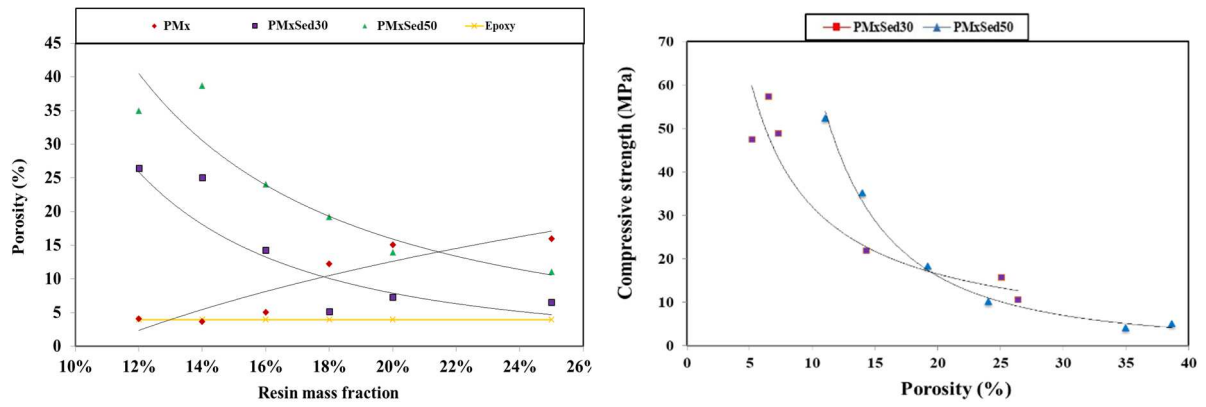


Figure 11. (a) Evolution of the porosity of the mortar PMx, PMxSed30 and PMxSed50 versus resin mass fraction; (b) the compressive strength as a function of the porosity

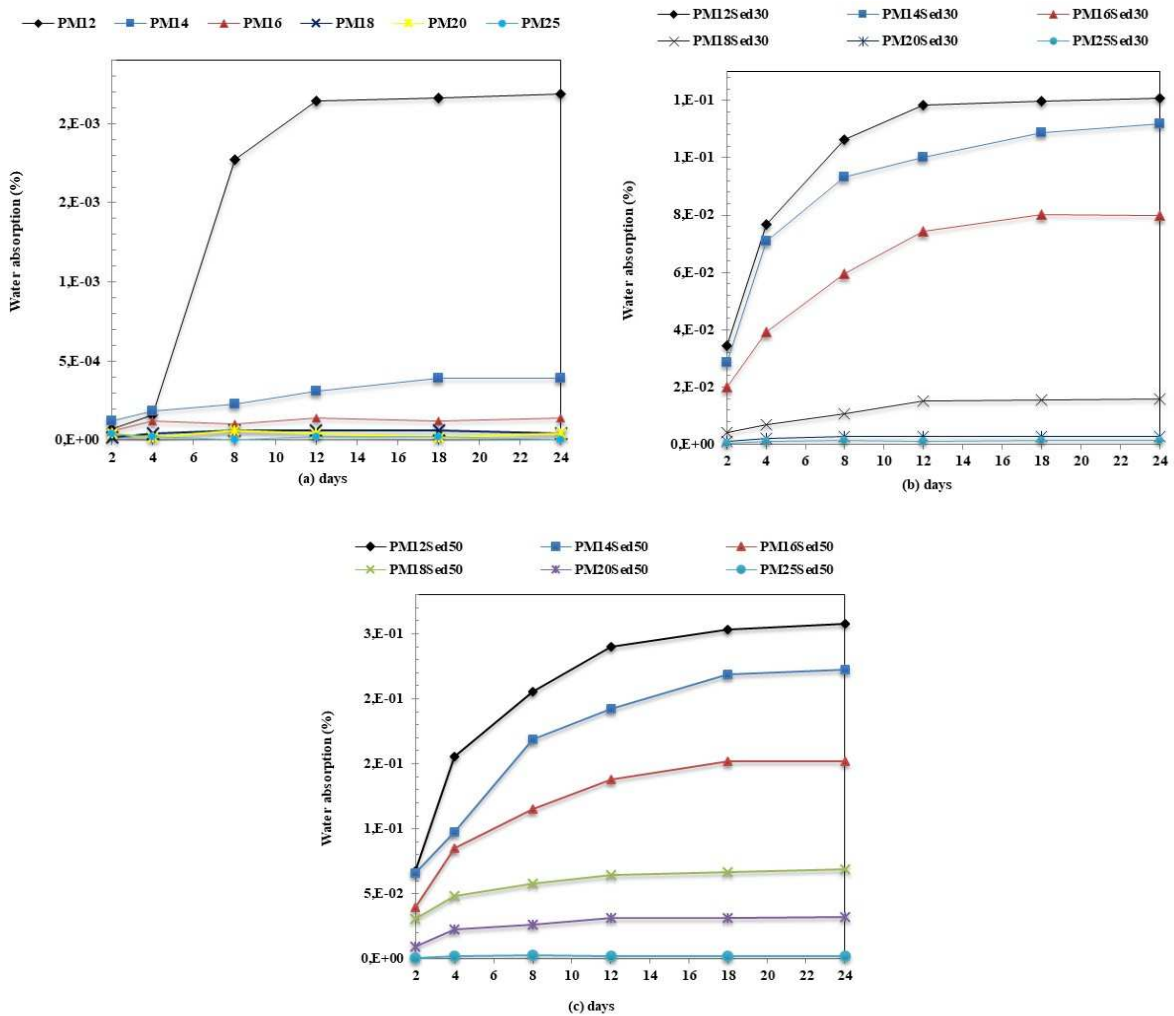


Figure 12. (a), (b) and (c) the water absorption of the PMx and PMxSed30, PMxSed50 mortar respectively as a function of curing time

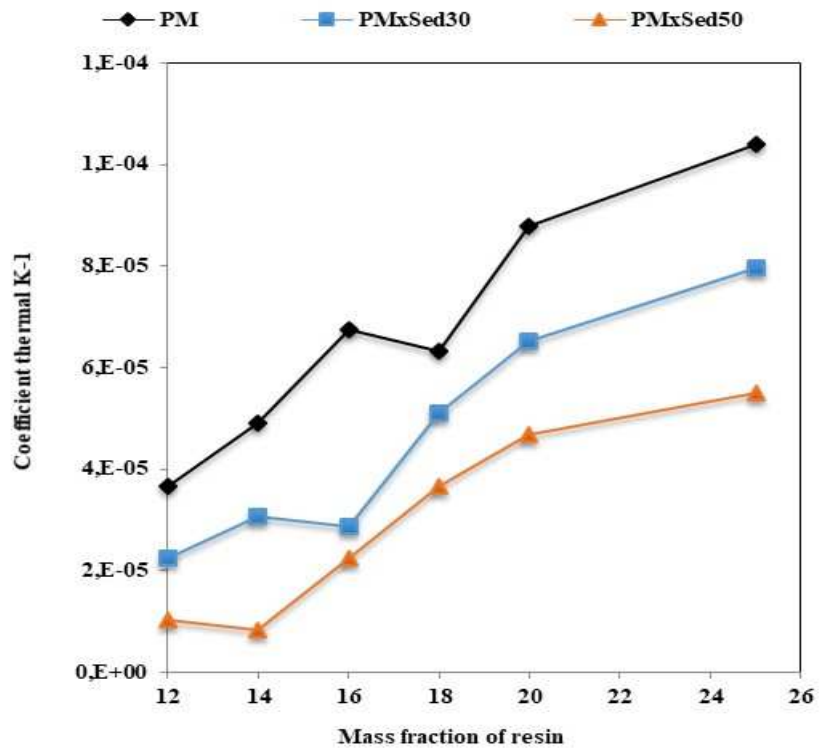
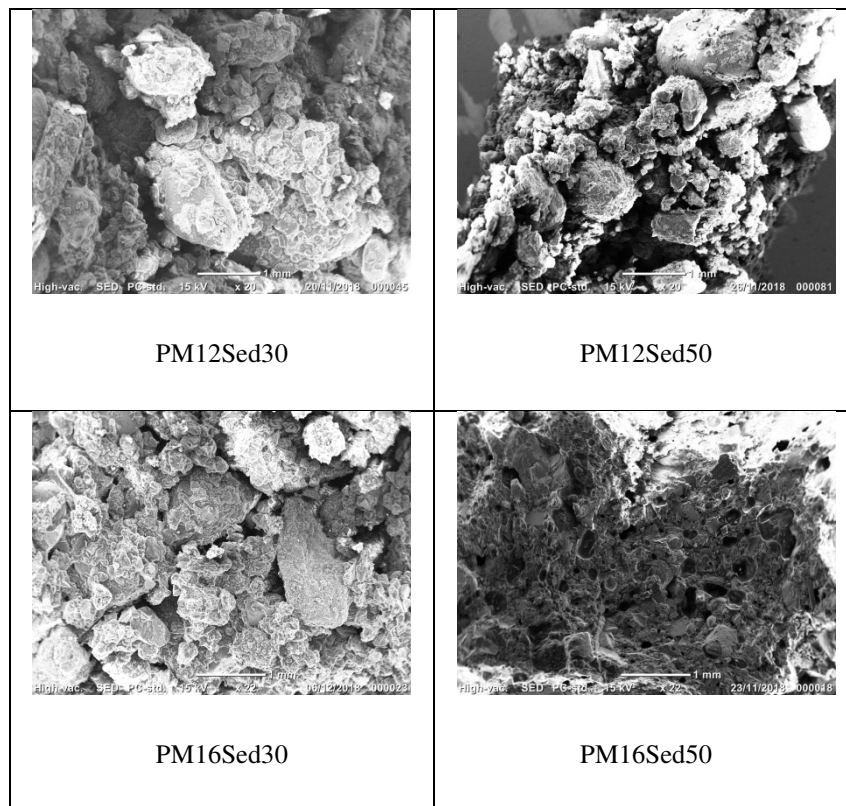


Figure 13. Evolution of the coefficient of thermal expansion of the PMx, PMxSed30 and PMxSed50



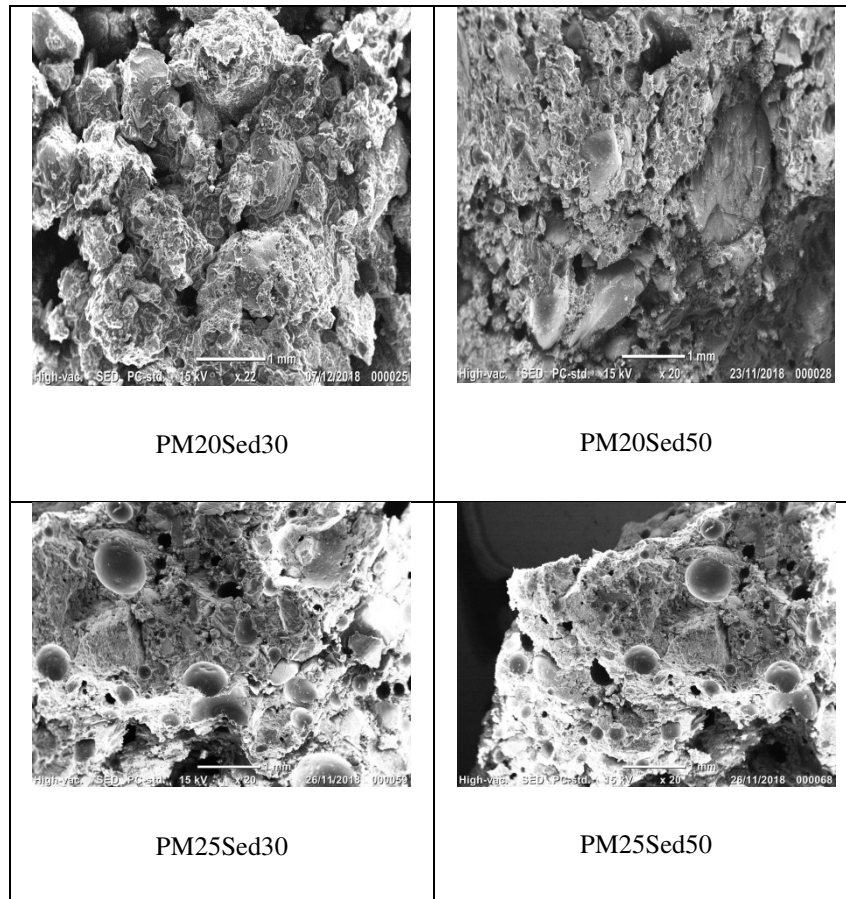


Figure 14. Scanning electron microscope (SEM) photograph from fracture surface of different formulation

Study of the polymer mortar based on dredged sediments and epoxy resin: Effect of the sediments on the behavior of the polymer mortar

Walid MAHERZI, Mahfoud BENZERZOUR, Ilyas ENNAHAL, Yannick MAMINDY-PAJANY, Nor-Edine ABRIAK

LGCgE-Laboratoire de Génie Civil et géoEnvironnement, Département Génie Civil and Environnemental, IMT Lille-Douai, Univ. Lille, EA 4515, 764 BD Lahure, 59500 Douai, France

Tables

Table 1. Characteristics of the used epoxy resin	2
Table 2. Characterization of the river sediments	2
Table 3. Elemental composition in X-ray fluorescence of the sediment.....	2
Table 4. the results of leaching of sediment and sand.....	2
Table 5. Polymer mortar formulations	3
Table 6. Results of leaching tests of mixtures PMxSed30	4
Table 7. Results of leaching tests of mixtures PMxSed50	5

Table 1. Characteristics of the used epoxy resin

Proportions of the mixture	Mix ratio resin to hardener => 2:1
Density	1.1 g / cm ³
Hardness Shore D	70 – 75
Hardness of the core	70 - 75 N / mm ² at 14 days
Heat resistance	+40 ° C to +45 ° C
Operating temperature	+10 ° C to +30 ° C
Viscosity	1000 - 1200 mPa.s

Table 2. Characterization of the river sediments

Characteristics	Standards	Sediment	Normal sand
density (Kg/m ³)	NF EN 1097-7	2610	2650
Methylene blue value (g/100 g of dry matter)	NF P 94-068	0.53	0.50
Organic matter content (%) at 450° C	XP P94-047	4.2	0.1
BET Surface (m ² /g)	NF EN ISO18757	11.0079	-

Table 3. Elemental composition in X-ray fluorescence of the sediment

Elements (%)	O	Na	Mg	Al	Si	P	S	Cl	K	Ca	Ti	Fe
Content	48,5	0,4	0,9	6,7	24,8	0,5	0,4	Traces	1,8	11,8	0,5	3,6

Table 4. the results of leaching of sediment and sand

Parameters	Sediment	Sand	ISDI threshold	ISDND threshold
As	0,1	< 0,1	0,5	2
Ba	3	0,03	20	100
Cd	0,01	< 0,01	0,04	1
Co	-	< 0,01	-	-
Cr	0,02	< 0,01	0,5	10
Cu	0,6	< 0,02	2	50
Hg	-	< 0,05	0,01	0,2
Mo	0,1	< 0,1	0,5	10
Ni	0,1	< 0,04	0,4	10
Pb	0,1	< 0,02	0,5	10
Sb	0,11	< 0,05	0,06	0,7
Se	0,07	< 0,11	0,1	0,5
Sn	-	< 0,06	-	-
V	-	0,03	-	-
Zn	1	< 0,03	4	50
chlorides	36	< 10	800	15000
fluorides	20	< 5	10	150
sulfates	270	< 10	1000	20000

soluble fraction	2837	358	4000	60000
pH	8,09	8,98	-	> 6
Conductivity ($\mu\text{S/cm}$)	264	27,75	-	-

Table 5. Polymer mortar formulations

Formulation	Epoxy resin (kg)	Sand (kg)	Sediment (kg)	Resin content in the mix. (%)
PM12	0.42	3.5	0	12
PM14	0.49	3.5	0	14
PM16	0.561	3.5	0	16
PM18	0.63	3.5	0	18
PM20	0.7	3.5	0	20
PM25	0.875	3.5	0	25
PM12Sed30	0.42	2.45	1.05	12
PM14Sed30	0.49	2.45	1.05	14
PM16Sed30	0.561	2.45	1.05	16
PM18Sed30	0.63	2.45	1.05	18
PM20Sed30	0.7	2.45	1.05	20
PM25Sed30	0.875	2.45	1.05	25
PM12Sed50	0.42	1.75	1.75	12
PM14Sed50	0.49	1.75	1.75	14
PM16Sed50	0.561	1.75	1.75	16
PM18Sed50	0.63	1.75	1.75	18
PM20Sed50	0.7	1.75	1.75	20
PM25Sed50	0.875	1.75	1.75	25

PMx: Polymer mortar with x the polymer content in (%) given by the total weight of the loads

PMxSedy: Polymer mortar with:

- X the polymer content in (%) given by the total weight of the loads.
- Y the sediment content in (%) given by the total weight of the loads.

Table 6. Results of leaching tests of mixtures PMxSed30

Parameters	Sediment	Sand	PM12 Sed30	PM14 Sed30	PM16 Sed30	PM18 Sed30	PM20 Sed30	PM25 Sed30	ISDI threshold	ISDND threshold
As	0,1	< 0,1	0,11	< 0,09	0,12	0,11	0,12	0,15	0,5	2
Ba	3	0,03	< 0,007	0,01	0,01	0,03	0,02	0,02	20	100
Cd	0,01	< 0,01	< 0,02	< 0,02	-	< 0,02	< 0,02	< 0,02	0,04	1
Co	-	< 0,01	0,14	0,12	0,11	0,16	0,26	0,17	-	-
Cr	0,02	< 0,01	< 0,004	< 0,004	-	< 0,004	< 0,004	< 0,004	0,5	10
Cu	0,6	< 0,02	< 0,007	0,07	-	< 0,007	< 0,007	< 0,007	2	50
Mo	0,1	< 0,1	< 0,04	< 0,04	-	< 0,04	< 0,04	< 0,04	0,5	10
Ni	0,1	< 0,04	< 0,03	< 0,03	-	< 0,03	< 0,03	< 0,03	0,4	10
Pb	0,1	< 0,02	< 0,09	< 0,09	-	< 0,09	< 0,09	< 0,09	0,5	10
Sb	0,11	< 0,05	< 0,2	< 0,2	-	< 0,2	< 0,2	< 0,2	0,06	0,7
Se	0,07	< 0,11	< 0,1	< 0,1	-	< 0,1	< 0,1	< 0,1	0,1	0,5
Sn	-	< 0,06	< 0,09	< 0,09	-	< 0,09	< 0,09	< 0,09	-	-
V	-	0,03	0,08	0,07	0,08	0,08	0,09	0,09	-	-
Zn	1	< 0,03	< 0,01	< 0,01	-	< 0,01	< 0,01	< 0,01	4	50
chlorides	36	< 10	< 10	12,5	15	30,5	36,5	24	800	15000
fluorides	20	< 5	7,25	5,7	4,05	4,15	4,3	4,55	10	150
sulfates	270	< 10	83,5	74,5	112,5	140	149,5	130,5	1000	20000
soluble fraction	2837	358	2103	3267	2614	4813	4338	4647	4000	60000
pH	8,09	8,98	8,48	8,65	8,83	8,76	8,77	8,71	-	> 6
Conductivity (µS/cm)	264	27,75	114,40	104,50	114,45	134,80	137,15	133,80	-	-

Table 7. Results of leaching tests of mixtures PMxSed50

Parameters	Sediment	Sand	PM12Sed50	PM14Sed50	PM16Sed50	PM18Sed50	PM20Sed50	PM25Sed50	ISDI threshold	ISDND threshold
As	0,1	< 0,1	0,19	0,14	0,13	0,16	0,13	0,16	0,5	2
Ba	3	0,03	0,03	< 0,007	0,01	< 0,007	0,02	0,03	20	100
Cd	0,01	< 0,01	< 0,02	< 0,02	< 0,02	< 0,02	< 0,02	< 0,02	0,04	1
Co	-	< 0,01	0,08	0,08	0,03	0,11	0,12	0,13	-	-
Cr	0,02	< 0,01	< 0,004	< 0,004	< 0,004	< 0,004	< 0,004	< 0,004	0,5	10
Cu	0,6	< 0,02	0,14	< 0,007	< 0,007	0,03	0,02	0,02	2	50
Mo	0,1	< 0,1	< 0,04	< 0,04	< 0,04	< 0,04	< 0,04	< 0,04	0,5	10
Ni	0,1	< 0,04	< 0,03	< 0,03	< 0,03	< 0,03	< 0,03	< 0,03	0,4	10
Pb	0,1	< 0,02	< 0,09	< 0,09	< 0,09	< 0,09	< 0,09	< 0,09	0,5	10
Sb	0,11	< 0,05	< 0,2	< 0,2	< 0,2	< 0,2	< 0,2	< 0,2	0,06	0,7
Se	0,07	< 0,11	< 0,1	< 0,1	0,07	0,08	0,09	0,13	0,1	0,5
Sn	-	< 0,06	< 0,09	< 0,09	< 0,09	< 0,09	< 0,09	< 0,09	-	-
V	-	0,03	0,13	0,11	0,08	0,09	0,09	0,1	-	-
Zn	1	< 0,03	0,03	< 0,01	< 0,01	< 0,01	< 0,01	< 0,01	4	50
chlorides	36	< 10	17,5	13	10,5	11,50	12	23,5	800	15000
fluorides	20	< 5	11,5	10	6	6,5	5,7	4,9	10	150
sulfates	270	< 10	165,5	141,5	163	175	180,5	191	1000	20000
soluble fraction	2837	358	3367	2857	3737	5656	2594	1362	4000	60000
pH	8,09	8,98	8,63	8,65	8,51	8,58	8,62	8,67	-	> 6
Conductivity (µS/cm)	264	27,75	152,25	143,15	133,95	141,95	144,00	155,70	-	-

Graphical abstract

